CASE FILE COPY

NACA

RESEARCH MEMORANDUM

ANALYTICAL AND EXPERIMENTAL STUDY OF TRANSIENT-RESPONSE CHARACTERISTICS OF A TURBOPROP ENGINE

By R. T. Craig, S. Nakanishi, and D. B. Wile

Lewis Flight Propulsion Laboratory
Cleveland, Ohio

NATIONAL ADVISORY COMMITTEE
FOR AERONAUTICS
WASHINGTON

October 21, 1955
Declassified July 17, 1958

NATIONAL ADVISORY COMMITTEE FOR AERONAUTICS

RESEARCH MEMORANDUM

ANALYTICAL AND EXPERIMENTAL STUDY OF TRANSIENT-RESPONSE CHARACTERISTICS OF A TURBOPROP ENGINE

By R. T. Craig, S. Nakanishi, and D. B. Wile

3527

SUMMARY

A turboprop engine was investigated over a range of Mach numbers from 0.15 to 0.5 at altitudes of 15,000 and 35,000 feet in order to obtain a description of the engine dynamic-response characteristics. Approximate step disturbances in the input variables, fuel flow and propeller blade angle, were utilized to obtain the desired information.

Engine response time was found to be affected by both altitude and Mach number. The rise ratios of the other variables considered, compressor-discharge pressure and torque, were only in part dependent on Mach number and were essentially unaffected by changes in altitude. Generalized engine gains also were dependent on flight conditions, and all dynamic characteristics changed with engine power level. A linearized first-order description of the engine response was found to be acceptable for propeller-blade-angle disturbances. Engine response for fuel-flow disturbances exhibited higher than first-order effects, but the causes of this were undetermined.

CE-1

INTRODUCTION

Design and analysis of the control systems for gas-turbine engines often can be simplified by use of analytical techniques in which part or all of the system is replaced with its mathematical equivalent. A particularly useful application of this procedure is to replace the engine with its dynamic equivalent thus permitting study of a complete controlled system without necessitating operation of a full-scale engine.

The choice of a mathematical representation of an engine largely will be determined by the modes of operation considered. If only stability and response to small perturbations are considered, a linearized first-order description of the engine can be useful. In order to obtain

information on this description of a turboprop engine, a number of experimental programs previously have been conducted, and the status of information available at the initiation of the investigation reported herein may be summarized as follows:

A turboprop engine, when subjected to a perturbation in either fuel flow or propeller blade angle, exhibits first-order linear characteristics up to at least 10-percent changes in speed, and the time constant can be closely predicted by calculation from steady-state characteristics (refs. 1 to 3). A limited frequency-response study of an engine over a range of altitudes at constant Mach number indicates that the generalized engine time constant is invariant with altitude (ref. 1). The effects of Mach number on the time constant have not been determined experimentally. Generalized engine gains such as speed to fuel flow $\left(\frac{\partial N}{\partial W}\right)_{\beta}\delta$ do not vary appreciably with changes in altitude, but Mach number effects on these gains have not been ascertained. The variations of torque- and compressor pressure-rise ratios with flight condition also have not been determined. Some differences have been noted between the response of a turboprop engine to a fuel-flow disturbance and a propeller-blade-angle disturbance, but the cause of these differences is undetermined. 3527

An experimental program was conducted in order to verify the existing information and to investigate further the dynamic performance of turboprop engines. The results of this program are presented in two reports - reference 4 and this report. The information presented in reference 4 may be summarized as follows:

Examination of engine rotational speed response at a 35,000-foot altitude over a range of Mach numbers showed a large variation in generalized time constant with Mach number. The time constants obtained from both fuel-flow and propeller-blade-angle disturbances showed similar trends with Mach number; however, the magnitude of the results from fuel-flow disturbances was considerably larger. The response times for blade-angle disturbances were predictable from knowledge of the engine and propeller steady-state characteristics, but only the general trends of the fuel-flow disturbance results could be predicted.

The objectives of this report are to present methods and information sufficient for a linearized dynamic description of the significant dependent and independent variables of a turboprop engine. The independent variables, fuel flow and propeller blade angle, and the dependent variables, torque, rotational speed, and compressor-discharge pressure, will be considered. Experimental information necessary to utilize the mathematical description is obtained and where possible is compared with results of previous investigations. Variations in engine

response with flight conditions are delineated as is the extent to which engine dynamic performance can be predicted by use of steady-state characteristics. Attention is paid to limitations of the first-order engine representation, and an effort is made to obtain a mathematical description of the differences in transient response that occur as different input variables are perturbated.

A turboprop engine was installed in the altitude wind tunnel of the NACA Lewis laboratory, and the dynamic characteristics were investigated over a range of Mach numbers from 0.15 to 0.5 at altitudes of 15,000 and 35,000 feet. The engine was subjected to perturbations in fuel flow and propeller blade angle of varied size and direction, and information sufficient for a dynamic-response description of the engine was obtained.

3527

ANALYSIS

If the analysis of the dynamic performance of a turboprop engine is limited to stability studies and to the response to small disturbances, a linearized treatment of the engine characteristics may be used. Since an engine has but one energy storage element, the propeller-engine rotor assembly, it can be considered a first-order system. This consideration, together with the assumption of quasistatic operation during a transient, results in the mathematical analysis presented in references 1 to 3. In these references it is shown that the speed response of a turboprop engine when disturbed by fuel flow and propeller blade angle is

$$\Delta N = \left(\frac{\partial N}{\partial W}\right)_\beta \left(\frac{1}{1 + \tau s}\right) \Delta W + \left(\frac{\partial N}{\partial \beta}\right)_W \left(\frac{1}{1 + \tau s}\right) \Delta\beta \tag{1}$$

(Symbols used are defined in appendix A.)

Other dependent variables such as torque, compressor-discharge pressure, and so forth, may be expressed in the general form X:

$$\Delta X = \left(\frac{\partial X}{\partial W}\right)_\beta \left(\frac{1 + a\tau s}{1 + \tau s}\right) \Delta W + \left(\frac{\partial X}{\partial \beta}\right)_W \left(\frac{1 + b\tau s}{1 + \tau s}\right) \Delta\beta \tag{2}$$

The same time constant τ appears in all these equations, and it may be expressed in partial-derivative form as

$$\tau = \frac{I_e + I_p}{\left(\frac{\partial Q}{\partial N}\right)_\beta + \left(\frac{\partial Q}{\partial N}\right)_W} \tag{3}$$

CE-1 back

All quantities are referred to the engine shaft speed by appropriate use of the reduction-gear ratio. The quantities a and b in equation (2) are rise ratios and also can be expressed in partial-derivative form as

$$a = 1 - \frac{\left(\frac{\partial N}{\partial W}\right)_{\beta} \left(\frac{\partial X}{\partial N}\right)_{W,\beta}}{\left(\frac{\partial X}{\partial W}\right)_{\beta}} \tag{4}$$

3527

and

$$b = 1 - \frac{\left(\frac{\partial N}{\partial B}\right)_{W} \left(\frac{\partial X}{\partial N}\right)_{W,\beta}}{\left(\frac{\partial X}{\partial \beta}\right)_{W}} \tag{5}$$

A more complete derivation of these equations is presented in appendix B. Depending on individual preference or convenience in a particular application, either the transfer-function or the partial-derivative presentation of these equations can be utilized. One convenient way of arranging the equations is the matrix form of figure 1. Here the engine inputs are shown at the top of each column. Output variables are obtained by taking the input to each column, multiplying it by the partial-derivative coefficients, and summing these products across the rows. Each row describes one dependent variable, and the first two columns show the direct effect of each independent variable on each dependent variable and thus are the gain terms of equations (1) and (2). The derivatives in column three are related to the rise ratios of equation (2) by the expressions of equations (4) and (5). For a turboprop engine all the terms in figure 1 generally can be evaluated by taking the slopes of the appropriate curves from steady-state performance maps. The extent to which the engine holds to quasistatic performance thus can be determined by comparison of the calculated response to the transient experimental results.

APPARATUS AND PROCEDURE

The turboprop engine utilized for the experimental program had a 19-stage axial-flow compressor, an eight-can combustor, and a four-stage turbine and was equipped with a three-blade 13-foot-diameter propeller. A complete description of the engine including the steady-state performance maps is given in reference 5. The engine was wing-mounted in the 20-foot-diameter test section of the NACA altitude wind tunnel as shown in figure 2.

Information on engine transient behavior was obtained through a program that consisted of approximate step changes in either fuel flow or propeller blade angle. Fuel-flow steps were obtained by an independent fuel system which consisted of the following: electrically driven pump, hydraulically actuated metering value, and a fast-acting regulator maintaining a constant pressure drop across the metering valve. For blade-angle disturbances the servo portion of the speed-pitch control system supplied with the propeller was utilized after modifications were made to obtain faster response. For each transient the engine and tunnel were allowed to reach equilibrium at a desired operating point, the disturbance was introduced, and the engine accelerated to a new equilibrium condition. Varied-size disturbances were introduced in each independent variable while the other independent variable was held constant at a desired value. Transients were run in pairs up from and down to a given point, and steady-state points were taken at the beginning and end of each transient.

Steady-state instrumentation was the standard wind-tunnel installation as described in reference 5. Transient information was obtained by use of three six-channel direct-inking strip-chart oscillographs with associated amplifiers for each channel. Table I gives the equipment used for both steady-state and transient measurement of each variable considered. Included in this table are the dynamic characteristics of the transient instrumentation. An engine cross section showing instrumentation stations is shown in figure 3.

RESULTS AND DISCUSSION

The turboprop-engine dynamic-response description in the matrix of figure 1 is a linear description of the engine, and the assumption is made that during a transient the engine will hold to quasistatic performance. Certain reservations on the validity of this description must be made, because the engine discussed herein is shown in reference 4 to exhibit differences in response characteristics that were dependent on which input variable, fuel flow or blade angle, was disturbed. After these reservations are recognized, an examination of the engine considered as a quasistatic system is possible. Information on the correctness, limitations, and uses of the engine description of figure 1 will be presented at appropriate points.

The presentation of results will be in this order: (1) engine experimental transient results for fuel-flow disturbances, (2) calculated engine response and comparison with experimental results of fuel-flow and blade-angle disturbances, (3) examination of variations between experimental and calculated results, and (4) development of modified engine description usable for this engine. In addition, an organization of engine information sufficient for a complete description of engine dynamics at the design flight condition is presented.

For convenience in making comparison, all engine information presented will be in generalized form. For this purpose standard NACA generalization factors, δ and θ, are utilized.

Engine Experimental Response to Fuel-Flow Disturbances

A typical experimental transient recording of engine response to a step change in fuel flow is shown in figure 4. The variables are fuel flow, propeller blade angle, torque, compressor-discharge pressure, engine rotational speed, turbine-inlet temperature, and tunnel dynamic pressure. The semilog method was used to determine time constants and rise ratios, and a typical response plot is shown in figure 5. Here the absolute value of each parameter in final steady state minus its value during the transient is plotted against time. The technique for obtaining time constants and rise ratios from such plots is given in reference 3.

Time Constant

The engine response times determined by the slopes of the semilog plots were obtained for a number of flight conditions and are shown in figures 6 and 7. In figure 6 the effects of Mach number and power level on the engine response time are shown for two altitudes. For both altitudes and at all power levels the generalized time constant is seen to increase as the Mach number decreases. The value at a Mach number of 0.15 is 60 percent larger than the value at a Mach number of 0.45. This change with Mach number, as developed in reference 4, can be predicted at a given altitude by the use of the propeller steady-state performance maps. Power level does have an effect on time constant, particularly at lower Mach numbers. At a Mach number of 0.15, the generalized time constant is about 50 percent greater at low power levels than it is in the range of high-power operation. As flight Mach number increases, the power-level effect lessens in significance; and at a Mach number of 0.45, the time constant at low power levels is only 20 percent greater than that at high power levels.

In the plot of figure 6, the data points shown were run at different values of propeller blade angle and rotational speed. A considerable effort was made to determine trends in the data scatter with each of these two variables, but none could be found. Varied-size fuel disturbances also were utilized to obtain the data in figure 6. The fuel disturbances were sufficient to cause from 4- to 10-percent changes in rotational speed, but in this range of inputs no trends with input disturbance size or direction could be discerned in the data scatter.

The effect of a change in altitude on the engine response time is illustrated in figure 7. Mach number is held constant in this plot, and

at both Mach numbers of 0.15 and 0.3 the generalized time constant is approximately 20 percent lower at an altitude of 35,000 feet than at 15,000 feet. This decrease conflicts with information obtained on previous turboprop and turbojet engines (ref. 6) where it was found that the generalized time constant was invariant with altitude. Further examination therefore was made of the engine steady-state performance characteristics.

In equation (3) it is seen that engine response time is dependent on the moments of inertia and two partial-derivative torque terms. One term $\left(\frac{\partial Q}{\partial N}\right)_\beta$ is a propeller characteristic and the other $\left(\frac{\partial Q}{\partial N}\right)_W$ is an engine characteristic. As mentioned previously, the engine considered herein also is the subject of reference 4, and in that report the propeller performance was shown to be predictable by use of the propeller-characteristic curves. The predicted performance indicated that at a given Mach number the gain $\left(\frac{\partial Q}{\partial N}\right)_\beta \frac{\sqrt{\theta}}{\delta}$ would not vary appreciably over a range of altitudes. Examination of the effects of gearbox losses on the derivatives as altitude changed showed that changes in the losses had negligible effect on the response time. Examination of the other partial derivative $\left(\frac{\partial Q}{\partial N}\right)_W \frac{\sqrt{\theta}}{\delta}$ requires constant fuel-flow information at the desired Mach number over a range of altitudes. This information is not available on the particular engine considered herein; however, such information is available from another of the same model that was the subject of reference 5. This report indicates that at a Mach number of 0.3 the slopes of constant-fuel-flow lines on generalized torque-speed maps are 60 percent steeper at 35,000 feet than they are at 15,000 feet. This increases $\left(\frac{\partial Q}{\partial N}\right)_W \frac{\sqrt{\theta}}{\delta}$ and, because of the relative size of the two torque terms involved, would decrease the generalized time constant approximately 20 percent. This is very close to the difference in the response times shown in figure 7.

Previous studies (refs. 1 and 6) have shown that the generalized speed response of a gas-turbine engine does not change appreciably with changes in altitude. The information presented herein, however, illustrates that at least one engine departs considerably from this expected performance. Therefore, it must be concluded that use of data from one flight condition to predict, through generalization, the speed response of an engine at another flight condition cannot be considered reliable. Generalization can be utilized to obtain a rough prediction of the characteristics of a specific engine at a desired flight condition. However, before these values can be considered to be reliable and accurate, data sufficient for at least a few point checks must be available from the particular flight condition studied.

Compressor-Discharge Pressure

The variations in compressor-discharge pressure-rise ratio with power level are shown in figures 8 and 9 for variations in altitude and Mach number, respectively. Figure 8 shows that the rise ratio increases with increasing power with about a 30-percent increase between low and high power. The variations in rise ratio with altitude are seen to be essentially negligible except at the low-power region at a Mach number of 0.15 (fig. 8(a)). Only one curve is drawn, but the data for an altitude of 15,000 feet have a tendency to be lower. This performance differs from the time-constant results where changes with altitude were noted. The speed response, and thus the time constant, is determined directly by relatively small differences in the large torques absorbed by the propeller and compressor and generated by the turbine. The compressor-discharge pressure-rise ratio is directly affected only by the combustion efficiency. Thus it is reasonable to expect that component efficiency changes with altitude that affect the generalized time constant will not necessarily affect the compressor-discharge pressure-rise ratio to a similar degree. If any such effects do appear, however, there is a possibility that they would be unnoticed, because the experimental determination of all rise ratios inherently has a greater degree of uncertainty than the time-constant determination.

In figure 9 are illustrated the effects of changes in Mach number on the pressure-rise ratio. At an altitude of 15,000 feet there is a slight increase in rise ratio for a change in Mach number from 0.15 to 0.3, while at 35,000 feet for the same Mach numbers there is no definite increase. The rise ratio at a Mach number of 0.45 and at 35,000 feet is higher than that at Mach numbers of 0.15 and 0.3, but at a Mach number of 0.5 the rise ratio tends toward the middle of the data. Because of these somewhat inconsistent effects of Mach number, single curves are drawn in figure 9. While it is not possible to specify the change in rise ratio with Mach number, a general trend of increase in rise ratio with increase in Mach number does exist. The order of magnitude of this observed increase is 10 to 30 percent over the range of Mach numbers tested. As in the case of the generalized time constant, no trends in the data scatter with the size or direction of the input disturbance could be determined.

Torque

The variation in torque-rise ratio with power level is shown in figures 10 and 11 for changes in Mach number and altitude, respectively. Figure 10 illustrates that at a constant Mach number the rise ratio is essentially independent of altitude and that the power level causes an increase in rise ratio of approximately 10 percent as operation progresses from low to high power. The nongeneralization of engine

characteristics (as brought forth under the time-constant discussion) also was expected to cause a change with altitude in the torque information, but none is observed. The degree of uncertainty in the rise-ratio results as discussed previously apparently masks any such result. Changes in Mach number also have little or no effect on the torque-rise ratio (fig. 11). This nonvariance can readily be explained by use of equation (4). In this equation let a be the torque-rise ratio and X be the torque. Even though the propeller torque characteristic $\left(\frac{\partial Q}{\partial W}\right)_\beta$ will change greatly with flight speed (ref. 4), its appearance in both numerator and denominator will minimize any effect on the rise ratio. Changes in $\left(\frac{\partial Q}{\partial N}\right)_W$ with Mach number could change the results but apparently do not. This term also is shown in reference 4 to be essentially invariant with Mach number at a given altitude.

Semilog reduction of experimental recordings of engine response characteristics to fuel-flow disturbances thus may be summarized as follows: Time constant decreases significantly and torque- and compressor-discharge pressure-rise ratios increase somewhat with increasing power level; torque- and pressure-rise ratios are essentially independent of altitude, while torque-rise ratio is essentially independent of and pressure is slightly dependent on Mach number. Time constant is affected significantly by both altitude and Mach number, and such trends are predictable by use of steady-state performance maps. In no case were any effects of input size and direction noticeable up to ±10-percent changes in speed, the maximum size studied.

Extent of Quasistatic Performance

The engine under consideration herein is shown in reference 4 to have response times for fuel-flow disturbances that were considerably longer than the response times that resulted from blade-angle disturbances. This performance differs from that typical of a linear first-order system; therefore, further investigation of the performance difference is in order

A comparison of engine time constants obtained in different ways is made. Time constants from blade-angle disturbances are obtained by use of numerical harmonic analysis (ref. 7), which was necessitated by the experimental blade inputs being too far from step form. Calculated time-constant values are obtained through use of torque-speed curves such as those of figure 12. The slopes of these curves are obtained and then substituted in equation (3). The generalized time constant from fuel-flow steps is obtained by use of the semilog method and is simply a transfer of the information of figure 6. Calculated values

3527

CE-2

of the time constant at various blade angles and rotational speeds are compared with those from blade-angle and fuel-flow transient data in figure 13 for two flight conditions. Blade-angle transient data are available only for an altitude of 35,000 feet. The time constants obtained from blade-angle transient data agree very closely with the calculated time constants, while those from fuel-flow transients are consistently 30 to 40 percent larger at both flight conditions. Thus the response to blade-angle disturbances may be considered to be quasistatic and predictable through the use of steady-state performance maps.

Comparison of compressor-discharge pressure-rise ratios requires steady-state maps such as that of figure 14. The slopes of the required curves are obtained and then substituted in the appropriate equations of the ANALYSIS section. The values obtained through point-by-point calculation are shown in figure 15, where calculated and experimental results are compared for two flight conditions. The experimental information is transferred from figures 8 and 9. A definite trend was noticeable in the calculated results with higher blade angles giving lower rise ratios. No similar trend took place in any of the transient experimental results. Therefore, in figure 15 a single curve is drawn through the calculated values for each flight condition. Comparison of each curve with the experimental results shows that the experimental results are approximately 65 to 85 percent of the calculated results at both flight conditions.

A similar examination of the torque-rise ratio is made in figure 16. Fuel-step data are obtained from figures 10 and 11, and calculated values are made with the use of steady-state maps such as that of figure 12. For this variable, as in the case of compressor pressure, the calculated results are considerably higher than the experimental values. The ratio between calculated and experimental values seems to remain fairly constant for both compressor-discharge pressure and torque and for both flight conditions.

Results of analysis of the fuel-step disturbances therefore are significantly different from the calculated, or what may be considered quasistatic, performance. Further examination of the results is in order. In figure 5 a typical semilog plot of speed, compressor-discharge pressure, and torque against time is shown. In such a plot each variable of a first-order linear system theoretically results in a number of intersecting straight lines with the line of finite slope determining the system time constant. In figure 5 the experimental results adhere closely to these lines over most of the plot, and only as the absolute values plotted go to zero is there a deviation of the experimental results from the theoretical values. This amount of deviation in itself is not significant. Closer results seldom can be obtained because of random errors in reading and recording. The significance, however, is

3527

that experimental results obtained on other engines produced a random variation above and below the theoretical line, while in the present case the experimental results invariably deviated upward from the theoretical lines as the plotted values approached zero. This indicated that some nonlinear or higher-order effects existed, but information on these effects could not be determined from examination of the semilog results. A number of fuel-step records, therefore, were analyzed by use of the numerical harmonic method previously used for blade-angle disturbances.

Typical results of this analysis are shown in figure 17. In figure 17(a) the amplitude ratio of speed to fuel flow is plotted against frequency. (All the amplitude ratios shown are divided by the zero-frequency amplitude ratio.) This figure does not show any unusual aspects, and the theoretical first-order curve agrees closely with the experimental results. In addition, the semilog and the harmonic-analysis methods give approximately the same response time as expressed by a time constant. Significant deviation from response typical of first-order systems is evidenced in figure 17(b), however. Here the phase shift of engine speed to fuel flow is plotted against frequency, and the experimental results show a phase shift in excess of the theoretical first-order curve drawn. The position of the first-order curve in figure 17(b) was obtained by placing its 45° phase-shift point at the same frequency as the 0.707 point of figure 17(a).

Examination of the engine experimental temperature response also gave evidence of unusual characteristics. The turbine-inlet-temperature trace in figure 4 is typical of the observed engine response to fuel steps and is significantly different from other engines considered previously. Figure 4 illustrates that after a fuel disturbance the temperature rose, decreased slightly, and then gradually increased to the final steady-state value. At no time during the initial portion of the transient does the temperature rise above the final steady-state value. Generally when an engine is subjected to a step increase in fuel flow, a sharp temperature rise immediately is expected and then as the speed, and thus the air flow, increases and exponentially approaches a steady-state final value, the temperature drops exponentially to a final value that is higher than the initial point. The experimental results shown in figure 4 obviously do not agree with this expected behavior. The consistent rise in temperature of the experimental response indicated that some long-term variation in the combustion process, a change in the efficiency of some component, or a change in the engine geometry was taking place with a change in fuel flow and thus causing the differences in response due to the different inputs. An obstacle to further examination encountered here was that both the harmonic and semilog methods tend to emphasize the zone in the time response close to the basic engine time constant. This emphasis plus normal data scatter (for

a gas-turbine engine) makes exceedingly difficult the determination of information that has characteristic times which differ from the basic engine time constant by more than a factor of 2 or 3.

The nature of the temperature trace indicates that a possible cause of the unusual engine behavior was that the combustion efficiency or the combustion zone changed during the transient, and this resulted in less than the expected amount of energy being available at the turbine to accelerate the engine. Temperature and fuel flow are closely connected; therefore it seemed reasonable to operate on the fuel-flow input to the engine by adding what could be considered dynamic combustion-efficiency terms.

3527

An effort was made to find what dynamic terms could be added to the engine description of figure 1 to result in closer agreement between calculated and experimental results. For this an analog computer was used, and the results are shown by the block diagram of figure 18. Here the input to the engine is effective fuel flow, and the mathematical expression relating it and actual fuel flow is considered an efficiency representation. The form of this mathematical expression was obtained by matching as closely as possible the simulated and experimental temperature traces. A typical simulated or calculated response is shown in figure 19(a), and examination of the temperature trace shows it to be very similar to the experimental recording of figure 4. Comparison of the experimental and simulated speed traces by use of harmonic analysis is made in figures 19(b) and (c). The data points are the fuel-step data of figure 17. In both figures the solid lines are the response of a first-order system to a true step input. The 1-second time constant of these curves was chosen arbitrarily during the process of obtaining the best possible match between the experimental and simulated temperatures. The dashed lines in figures 19(b) and (c) are the response of the same 1-second engine to the effective-fuel-flow input. They show in the frequency domain the simulated response that was shown in the time domain in figure 19(a). Agreement between the simulated response to effective fuel flow and the experimental response to actual flow is good both in amplitude ratio and phase shift.

Since the simulated and experimental responses match, it is of interest to note the differences in effective response times in figure 19(b). (Response time is considered to be determined by the 0.707 amplitude-ratio point.) The effective response time of the 1-second engine increases 35 percent when subjected to the effective fuel input rather than to a true step input. This percentage difference is essentially the same magnitude as that shown between fuel-flow and blade-angle results in figure 13. This percentage difference also is the result that would be obtained by different inputs to the matrix engine description of figure 18. Thus the addition of the effective-fuel-flow dynamic terms (fig. 18) produces an engine description that does the

following: (1) causes the experimental and simulated temperature traces to be very similar, (2) produces simulated speed traces that match experimental results, and (3) allows the simulated engine to have response times to fuel-flow disturbances that are considerably longer than the response times to blade-angle disturbances.

An adequate description of the rotational-speed response of this engine to fuel-flow disturbances thus requires the first-order terms of the basic engine plus additional dynamic terms such as those introduced through the effective-fuel-flow concept. An adequate description of the engine response of propeller-blade-angle disturbances requires only the first-order terms of the basic engine.

For the other variables such as torque and pressure that have rise ratios in their transient descriptions, the dynamics of effective fuel flow also will affect the description of the engine response. The dynamic relation of effective fuel flow to actual fuel flow is, from figure 18,

$$\Delta W_{ef} = \frac{1 + c\tau_W s}{(1 + \tau_W s)(1 + 0.03\tau_W s)} \Delta W \tag{6}$$

Hence the experimental transient recording of a response to a fuel-step disturbance would not be that of equation (2) but would be

$$\Delta X = \left(\frac{\partial X}{\partial W}\right)_\beta \frac{(1 + a\tau s)}{(1 + \tau s)} \left[\frac{1 + c\tau_W s}{(1 + \tau_W s)(1 + 0.03\tau_W s)}\right] \Delta W \tag{7}$$

The experimental rise ratios were determined by the semilog method. This procedure minimizes the effects of any time terms that are short relative to the engine time constant. The experimental initial rise in X upon a fuel disturbance therefore would be the limit of equation (7) as time approached zero but excluding the term $(1 + 0.03\tau_W s)$; that is,

$$\Delta X = \left(\frac{\partial X}{\partial W}\right)_\beta (ac)\Delta W$$

The rise ratio as calculated from equation (4) and the steady-state performance maps is a. Thus, if the effective-fuel-flow concept is reasonable, the experimental transient results will appear, in comparison with calculated results, too small by the amount of the rise ratio c of equation (6)(again with the exclusion of the effects of the term $(1 + 0.03\tau_W s)$). The rise-ratio comparison plots of figures 15 and 16 show that all the experimental results are about 75 to 85 percent of

the calculated results. The effective-fuel-flow concept thus is substantiated by the torque- and pressure-rise-ratio information as well as by the speed and temperature information discussed previously.

Separate examination of the speed, pressure, and torque responses thus consistently indicates that, when fuel-flow disturbances to this engine are considered, the calculated or predicted transient response can be correlated with the actual experimental results by addition of dynamic terms such as those of effective fuel flow in equation (6). Because of experimental scatter, it was impossible from comparison with the analog results to define clearly these additional dynamics, but the form of equation (6) is a reasonable approximation. The rise ratio c is in the range of 0.75 to 0.85 and τ_W is about five times the engine time constant. Use of these values for this engine will give good agreement between the calculated and experimental results. This agreement will hold for time constants and rise ratios and for fuel and blade-angle inputs.

3527

Correlation of the results is not a proof of the effective-fuel-flow concept. It merely illustrates that, in the frequency range considered, agreement can be obtained between the experimental and calculated results by adding a number of dynamic terms to the fuel input. The description of these terms as obtained (eq. (6)) is simple and only may be an approximation of more complex phenomenon. Consideration of the dynamic approximation of equation (6) does, however, provide the controls-system designer for this particular engine with a more accurate computational method than would be available with the engine description of figure 1 alone. A more rigorous and exact analysis of these additional dynamics would be desirable, but more consistent data over the frequency range already studied and data usable over a wider frequency range than presently available would be necessary. Such data also might provide an insight to the exact cause and nature of the phenomena.

The preceding analysis of adding dynamic terms to the input of the system, while reasonable, is not the only possibility. Effects similar to those accounted for by equation (6) also may be introduced by a change in the engine internal geometry or a change in the turbine flow processes as the temperature level is changed with fuel flow. Various details of engine design were examined for explanations, and just one seemed significant. The transport time of a gas particle through the combustion chamber (obtained by dividing the length of the chamber by the average gas velocity) was determined for this and for other engines previously studied. The engine discussed herein comparatively had less time to complete the combustion process within the chamber, and this may have been a contributing factor to the unusual behavior encountered.

Engine Gain Terms

In equations (1) and (2), which describe an engine transient response, the terms $\left(\frac{\partial X}{\partial W}\right)_\beta$, $\left(\frac{\partial X}{\partial \beta}\right)_W$, $\left(\frac{\partial N}{\partial W}\right)_\beta$, and $\left(\frac{\partial N}{\partial \beta}\right)_W$ are frequency or time independent quantities and are usually termed gains. As such they are the portion of the engine characteristic that would enter into the overall gain of a control loop, and they appear in the first two columns of figures 1 and 18. It is of interest to determine how these coefficients vary with engine operation point and flight condition. Complete operation maps are available only for an altitude of 15,000 feet and a Mach number of 0.3 and for an altitude of 35,000 feet and a Mach number of 0.45. From these maps the slopes are obtained and those for compressor-discharge pressure are shown in figure 20. In figures 20(a) and (b) the gains $\left(\frac{\partial P_3}{\partial W}\right)_\beta \sqrt{\theta}$ are shown for two flight conditions. Variations with power level and propeller blade angle readily can be seen. In addition, the generalized gains at 35,000 feet are considerably lower than those at 15,000 feet. The variations with propeller blade angle at 35,000 feet also are more pronounced, although this may be due to the larger blade angles and the larger rotational-speed changes that occur at higher Mach numbers. In figures 20(c) and (d) the gains $\left(\frac{\partial P_3}{\partial \beta}\right)_W \frac{1}{\delta}$ are shown, and these also show decided differences at the two flight conditions. These variations are typical of those encountered for all other variables considered, and therefore it can be concluded that the generalized engine gains vary significantly with altitude and Mach number. Knowledge of the change in propeller characteristics with Mach number makes it seem probable that most of the differences shown in figure 20 are due to Mach number rather than to altitude effects, but data sufficient for proof are not available.

Presentation of the speed and torque gains to fuel flow and propeller blade angle will complete the matrix representation of the engine at 15,000 feet and a Mach number of 0.3. These gains are shown in figures 21 and 22. As in the case of compressor-discharge pressure, both the speed and torque gains show decided variations with power level and blade angle.

Since the generalized gains vary with flight condition as do the time constants and some rise ratios, the engine description will be completed only for an altitude of 15,000 feet and a Mach number of 0.3, which is the approximately design point of the engine.

3527

It also is helpful to present the rise-ratio information of figures 15 and 16 in the partial-derivative form that is directly applicable to the matrix of figure 18. This is done in figure 23, where the gains $\left(\frac{\partial Q}{\partial N}\right)_W \frac{\sqrt{\theta}}{\delta}$ and $\left(\frac{\partial P_3}{\partial N}\right)_W \frac{\sqrt{\theta}}{\delta}$ are shown plotted against generalized shaft horsepower.

Use of figures 13 and 20 to 23 thus provides information sufficient for a description of the dynamic response of this turboprop engine over the entire operation range at an altitude of 15,000 feet and a Mach number of 0.3. Considerable changes must be expected in all quantities if the flight condition is changed. For convenience, values at 100-percent power at 15,000 feet and a Mach number of 0.3 are tabulated in table II.

SUMMARY OF RESULTS

A turboprop engine was investigated over a range of Mach numbers from 0.15 to 0.5 at altitudes of 15,000 and 35,000 feet. A description of the engine dynamic response is presented for an altitude of 15,000 feet and a Mach number of 0.3.

The extent that the generalized time constant varied with Mach number was delineated. The generalized time constant at a Mach number of 0.15 was found to be 60 percent larger than the value at a Mach number of 0.45. The generalized time constant also varied with altitude and power level. Values at 35,000 feet were approximately 20 percent lower than those at 15,000 feet. This variation was found to be predictable by use of the steady-state performance maps at each flight condition.

Rise ratios of torque and compressor-discharge pressure for fuel-step inputs increased slightly with increasing power level but did not change appreciably as altitude varied. Torque-rise ratio did not vary appreciably with Mach number, but compressor-discharge pressure-rise ratio did increase slightly with increasing Mach number.

Engine response to blade-angle disturbances was found to be first order and quasistatic and is predictable through the use of the slopes of steady-state performance maps.

Engine response to fuel-flow disturbances was found to have higher than first-order effects. In comparison with calculated quasistatic results, experimental results were slower in time response and smaller for each rise ratio. Differences in response were mathematically approximated, but causes of these differences were not determined. Possible causes seemed to be changes in the combustion process or changes in engine internal geometry or flow conditions with power level.

The characteristics of the engine dynamic response were found to be unaffected by the size or direction of the input disturbance. Disturbances causing 4- to 10-percent changes in rotational speed were utilized.

Lewis Flight Propulsion Laboratory
National Advisory Committee for Aeronautics
Cleveland, Ohio, March 31, 1955

APPENDIX A

SYMBOLS

The following symbols are used in this report:

a,b,c	rise ratios
I_e	engine rotor polar moment of inertia referred to engine shaft
I_p	propeller polar moment of inertia referred to engine shaft
N	engine rotational speed
P	pressure
Q	shaft torque
s	Laplace operator
shp	shaft horsepower
W	fuel flow
W_{ef}	effective fuel flow
X	general dependent variable
$\left(\frac{\partial X}{\partial W}\right)_\beta$	partial derivative of X with respect to fuel flow with propeller blade angle constant
β	propeller blade angle
δ	ratio of absolute total pressure to NACA standard pressure at sea-level static conditions
θ	ratio of absolute total temperature to NACA standard temperature at sea-level static conditions
τ	time constant of engine-propeller combination
τ_W	time constant of effective fuel flow

Subscripts:

e	engine

3527

f	final value
p	propeller
1	engine inlet
2	compressor inlet
3	compressor discharge
4	turbine inlet
5	tail pipe

3527

APPENDIX B

DERIVATION OF TRANSIENT-RESPONSE EQUATIONS

The equations governing engine transient response are developed on the basis of the assumptions that the engine is first order, that it can be linearized about an operating point, and that all performance is quasistatic.

Engine torque is assumed to be a function of fuel flow and speed:

$$Q_e = Q(W,N)$$

For small excursions around a point,

$$\Delta Q_e = \left(\frac{\partial Q}{\partial W}\right)_N \Delta W + \left(\frac{\partial Q}{\partial N}\right)_W \Delta N$$

The difference between engine torque and shaft torque accelerates the engine. Thus,

$$\Delta Q_e - \Delta Q = I_e \Delta N s$$

In a similar manner, propeller torque is assumed to be a function of blade angle and speed:

$$Q_p = Q(\beta,N)$$

Propeller torque also can be expanded for excursions around a point.

The expanded expressions can be combined and the shaft torque eliminated. Then at constant blade angle,

$$\left(\frac{\partial Q_e}{\partial W}\right)_N \Delta W = \left[(I_p + I_e)s + \left(\frac{-\partial Q_e}{\partial N}\right)_W + \left(\frac{\partial Q_p}{\partial N}\right)_\beta\right]\Delta N$$

This expression can be rewritten as

$$\left(\frac{\Delta N}{\Delta W}\right)_\beta = \frac{\left(\frac{\partial Q_e}{\partial W}\right)_N}{\left(\frac{-\partial Q_e}{\partial N}\right)_W + \left(\frac{\partial Q_p}{\partial N}\right)_\beta + (I_p + I_e)s}$$

or in the form

$$\left(\frac{\Delta N}{\Delta W}\right)_\beta = \left(\frac{\partial N}{\partial W}\right)_\beta \left(\frac{1}{1 + \tau s}\right)$$

where

$$\tau = \frac{I_p + I_e}{\left(\frac{-\partial Q_e}{\partial N}\right)_W + \left(\frac{\partial Q_p}{\partial N}\right)_\beta}$$

and

$$\left(\frac{\partial N}{\partial W}\right)_\beta = \frac{\left(\frac{\partial Q_e}{\partial W}\right)_N}{\left(\frac{-\partial Q_e}{\partial N}\right)_W + \left(\frac{\partial Q_p}{\partial N}\right)_\beta}$$

If fuel flow is held constant, the speed response to blade angle can be obtained as

$$\left(\frac{\Delta N}{\Delta \beta}\right)_W = \frac{\left(\frac{-\partial Q_p}{\partial \beta}\right)_N}{\left(\frac{-\partial Q_e}{\partial N}\right)_W + \left(\frac{\partial Q_p}{\partial N}\right)_\beta + (I_p + I_e)s}$$

or in the form

$$\left(\frac{\Delta N}{\Delta \beta}\right)_W = \left(\frac{\partial N}{\partial \beta}\right)_W \left(\frac{1}{1 + \tau s}\right)$$

where

$$\left(\frac{\partial N}{\partial \beta}\right)_N = \frac{\left(\frac{-\partial Q_p}{\partial \beta}\right)_N}{\left(\frac{-\partial Q_e}{\partial N}\right)_W + \left(\frac{\partial Q_p}{\partial N}\right)_\beta}$$

Speed response to both fuel-flow and blade-angle disturbances is

$$\Delta N = \left(\frac{\partial N}{\partial W}\right)_\beta \left(\frac{1}{1 + \tau s}\right) \Delta W + \left(\frac{\partial N}{\partial \beta}\right)_W \left(\frac{1}{1 + \tau s}\right) \Delta \beta$$

Any other engine variable X is assumed to be a function of fuel flow and speed:

$$X = X(W,N)$$

$$\Delta X = \left(\frac{\partial X}{\partial W}\right)_N \Delta W - \left(\frac{\partial X}{\partial N}\right)_W \Delta N$$

At constant blade angle, substitution of the previously obtained value for ΔN gives

3527

$$\Delta X = \left(\frac{\partial X}{\partial W}\right)_N \Delta W - \left(\frac{\partial X}{\partial N}\right)_W \left(\frac{\partial N}{\partial W}\right)_\beta \left(\frac{1}{1 + \tau s}\right)\Delta W$$

or

$$\left(\frac{\Delta X}{\Delta W}\right)_\beta = \frac{\left(\frac{\partial X}{\partial W}\right)_N - \left(\frac{\partial N}{\partial W}\right)_\beta \left(\frac{\partial X}{\partial N}\right)_W + \left(\frac{\partial X}{\partial W}\right)_N \tau s}{1 + \tau s}$$

This also can be written in the form

$$\left(\frac{\Delta X}{\Delta W}\right)_\beta = \left(\frac{\partial X}{\partial W}\right)_\beta \left(\frac{1 + a\tau s}{1 + \tau s}\right)$$

where

$$\left(\frac{\partial X}{\partial W}\right)_\beta = \left(\frac{\partial X}{\partial W}\right)_N - \left(\frac{\partial N}{\partial W}\right)_\beta \left(\frac{\partial X}{\partial N}\right)_W$$

and

$$a = \frac{\left(\frac{\partial X}{\partial W}\right)_N}{\left(\frac{\partial X}{\partial W}\right)_\beta}$$

If fuel flow is held constant and blade angle is varied, the previous expression for the expansion of X becomes

$$\Delta X = - \left(\frac{\partial X}{\partial N}\right)_W \Delta N$$

Substituting for ΔN results in

$$\left(\frac{\Delta X}{\Delta \beta}\right)_W = \left(\frac{\partial X}{\partial N}\right)_W \left(\frac{\partial N}{\partial \beta}\right)_W \left(\frac{1}{1 + \tau s}\right)$$

and

$$\left(\frac{\partial X}{\partial \beta}\right)_W = \left(\frac{\partial X}{\partial N}\right)_W \left(\frac{\partial N}{\partial \beta}\right)_W$$

3527

The final expression for the variable X thus can be written as

$$\Delta X = \left(\frac{\partial X}{\partial W}\right)_\beta \left(\frac{1 + a\tau s}{1 + \tau s}\right) \Delta W + \left(\frac{\partial X}{\partial \beta}\right)_W \left(\frac{1}{1 + \tau s}\right) \Delta \beta$$

REFERENCES

1. Krebs, Richard P., Himmel, Seymour C., Blivas, Darnold, and Shames, Harold: Dynamic Investigation of Turbine-Propeller Engine under Altitude Conditions. NACA RM E50J24, 1950.

2. Taylor, Burt L., III, and Oppenheimer, Frank L.: Investigation of Frequency-Response Characteristics of Engine Speed for a Typical Turbine-Propeller Engine. NACA Rep. 1017, 1951. (Supersedes NACA TN 2184.)

3. Oppenheimer, Frank L., and Jacques, James R.: Investigation of Dynamic Characteristics of a Turbine-Propeller Engine. NACA RM E51F15, 1951.

4. Nakanishi, S., Craig, R. T., and Wile, D. B.: Effect of Flight Speed on Dynamics of a Turboprop Engine. NACA RM E55A05, 1955.

5. Essig, R. H., and Schulze, F. W.: Altitude Performance and Operational Characteristics of an XT38-A-2 Turboprop Engine. NACA RM E53L18a, 1954.

6. Craig, R. T., Vasu, George, and Schmidt, R. D.: Dynamic Characteristics of a Single-Spool Turbojet Engine. NACA RM E53C17, 1953.

7. Delio, Gene J.: Evaluation of Three Methods for Determining Dynamic Characteristics of a Turbojet Engine. NACA TN 2634, 1952.

3527

TABLE I. - INSTRUMENTATION

Measured quantity	Steady-state instrumentation	Transient instrumentation	
		Sensor	Frequency range, cps
Fuel flow	Rotameter	Aneroid-type pressure sensor, with strain-gage element, connected to measure pressure drop across variable orifice in fuel line	0 to 20
Blade angle	Slide-wire on propeller and connected in electrical circuit to give indication on microammeter	Slide-wire on propeller	0 to 100
Engine speed	Modified electronic digital counter with frequency-generating tachometer	Shaped frequency signal from counter integrated with respect to time	0 to 35
Thrust	Calibrated bridge balance on strain analyzer	Strain gage and link attached to engine mounting frame	0 to 50
Torque	Electronic measurement with reluctance pickups of twist in drive shaft between compressor and gearbox. Indication of twist given on calibrated self-balancing potentiometer	Torquemeter modified to give transient indication	0 to 60
Turbine-inlet temperature	Nine individual thermocouples connected to self-balancing recorder	Four paralleled 20-gage chromel-alumel thermocouples and electric network to compensate for thermocouple lag	0 to 25 at sea level when used with properly adjusted compensator
Turbine-outlet temperature	Sixteen individual thermocouples connected to self-balancing recorder	Eight paralleled 20-gage chromel-alumel thermocouples and electric network to compensate for thermocouple lag	0 to 15 at sea level when used with properly adjusted compensator
Tunnel dynamic pressure	Water manometers	Aneroid-type pressure sensor, with strain-gage element	Damping ratio of 0.5, and damped natural frequency of 20 cps at 15,000 ft
Engine air flow	Water manometers	Diaphragm-type pressure sensor, with strain-gage element	Damping ratio of 0.5, and damped natural frequency of 20 cps at 15,000 ft
Compressor-inlet total pressure	Water manometers	Diaphragm-type pressure sensor, with strain-gage element	
Compressor-outlet total pressure	Mercury manometers	Aneroid-type pressure sensor, with strain-gage element	

TABLE II. - ENGINE COEFFICIENTS FOR MATRIX OF FIGURE 18

[Coefficients evaluated at 100-percent power[a] at altitude of 15,000 ft and Mach number of 0.3]

$\tau_s/\sqrt{\theta}$, sec	0.68
$\left(\frac{\partial N}{\partial W}\right)_\beta \delta$, rpm/(lb/hr)	2.3
$\left(\frac{\partial N}{\partial \beta}\right)_W \frac{1}{\sqrt{\theta}}$, rpm/deg	-400
$\left(\frac{\partial Q}{\partial W}\right)_\beta \sqrt{\theta}$, lb-ft/(lb/hr)	0.644
$\left(\frac{\partial Q}{\partial \beta}\right)_W \frac{1}{\delta}$, lb-ft/deg	44.5
$\left(\frac{\partial Q}{\partial N}\right)_W \frac{\sqrt{\theta}}{\delta}$, lb-ft/rpm	-0.17
Torque-rise ratio	0.42
$\left(\frac{\partial P_3}{\partial W}\right)_\beta \sqrt{\theta}$, (lb/sq ft)/(lb/hr)	4.4
$\left(\frac{\partial P_3}{\partial \beta}\right)_W \frac{1}{\delta}$, (lb/sq ft)/deg	-320
$\left(\frac{\partial P_3}{\partial N}\right)_W \frac{\sqrt{\theta}}{\delta}$, (lb/sq ft)/rpm	0.97
Compressor-discharge pressure-rise ratio	0.40
$\tau_W = 5\tau\delta/\sqrt{\theta}$, sec	3.4
c	0.8

[a]Steady-state engine conditions at 100-percent power are: β, 42.0°; $W/\delta\sqrt{\theta}$, 1640 lb/hr; $shp/\delta\sqrt{\theta}$, 2520 hp; $N/\sqrt{\theta}$, 14,200 rpm.

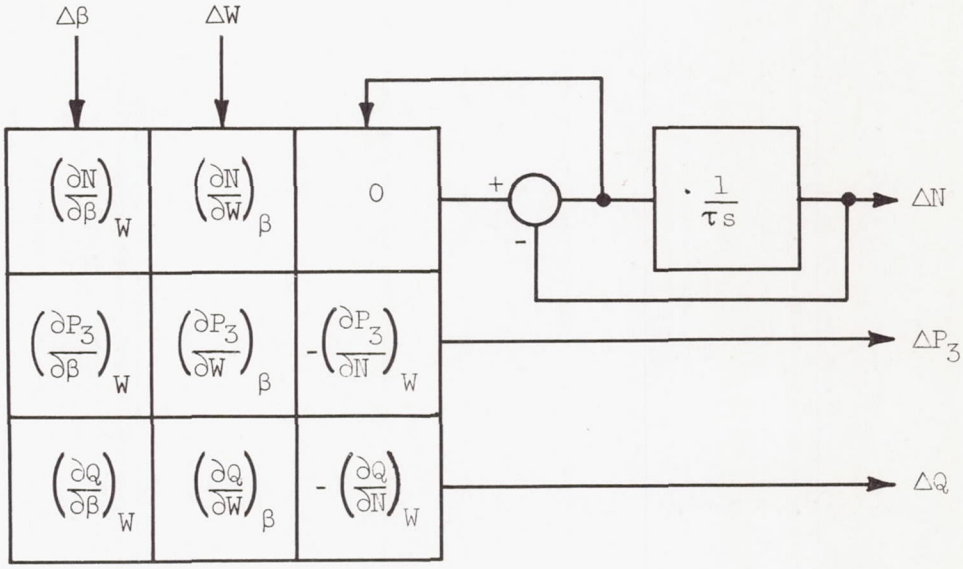

Figure 1. - Matrix form used in linear first-order description of dynamic-response characteristics of turboprop engine.

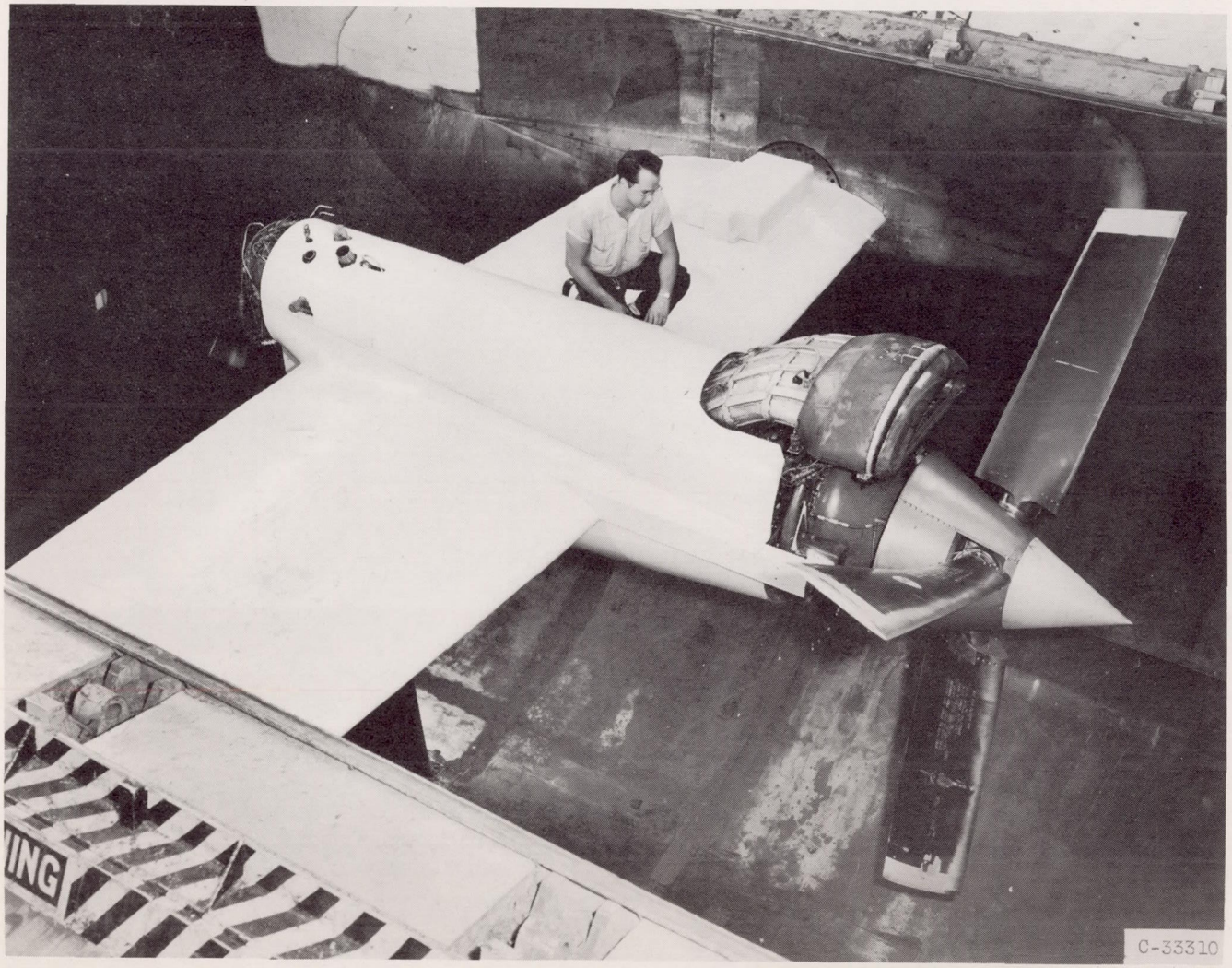

Figure 2. - Installation of turboprop engine in altitude wind tunnel.

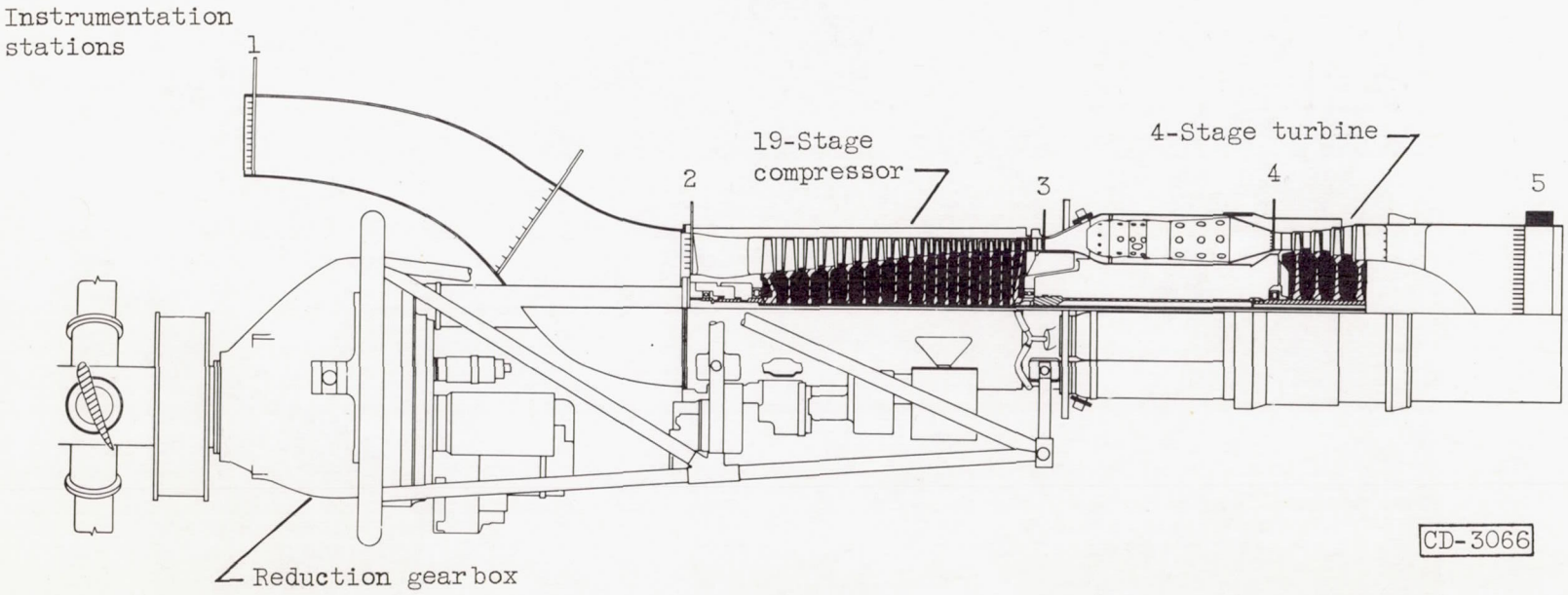

Figure 3.- Cross section of engine showing components and instrumentation stations.

3527

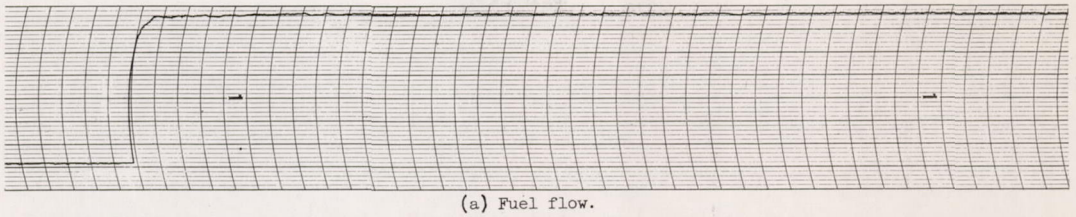

(a) Fuel flow.

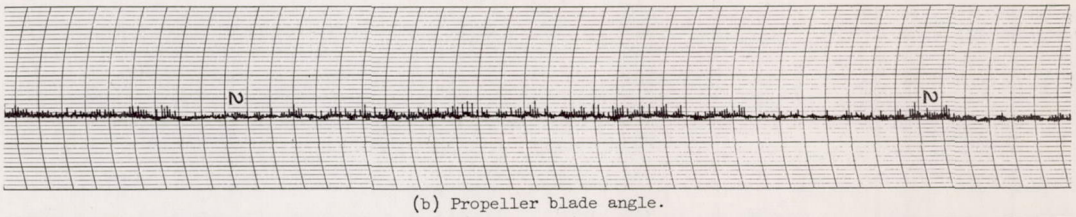

(b) Propeller blade angle.

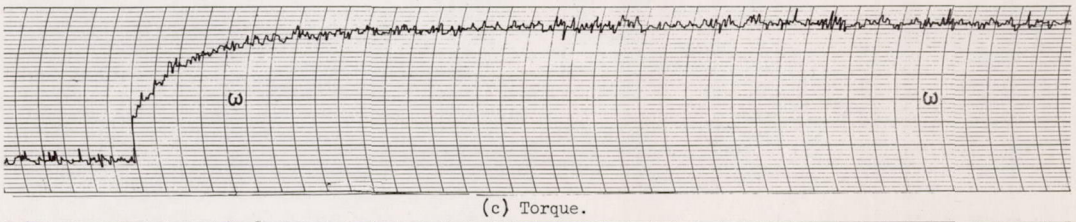

(c) Torque.

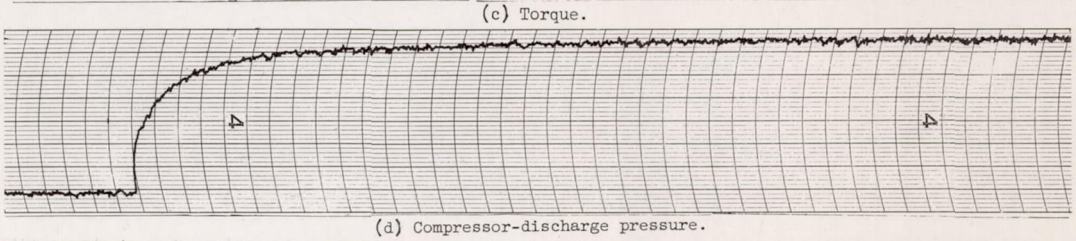

(d) Compressor-discharge pressure.

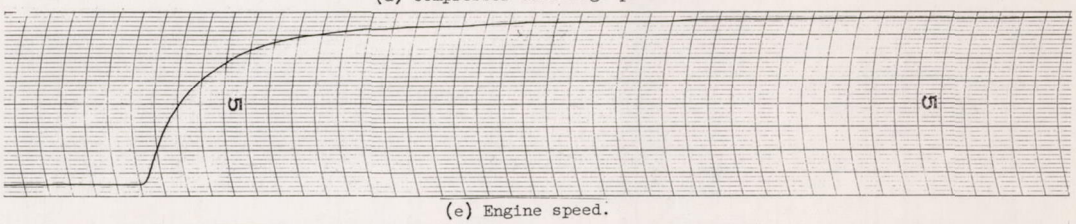

(e) Engine speed.

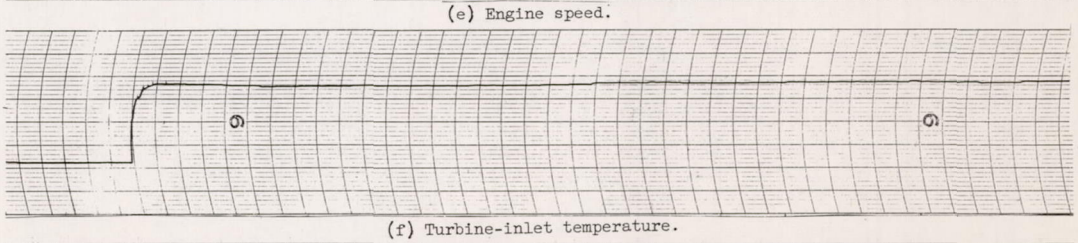

(f) Turbine-inlet temperature.

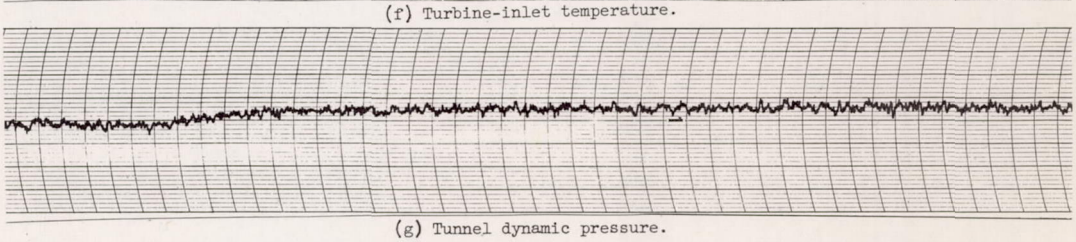

(g) Tunnel dynamic pressure.

Figure 4. - Experimental transient recording of engine response to fuel-flow step disturbance. Altitude, 35,000 feet; Mach number, 0.45.

3527

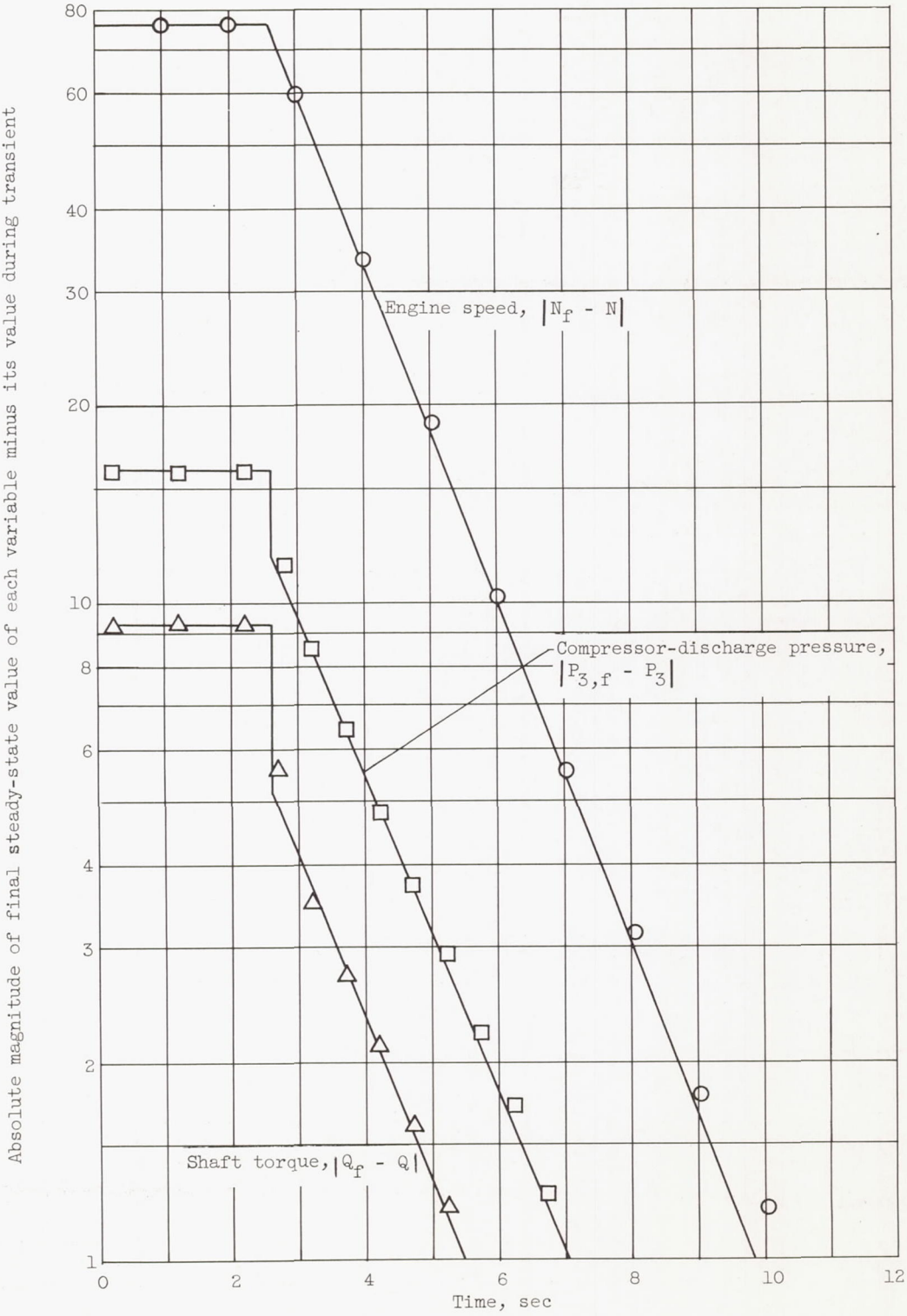

Figure 5. - Semilog plot of engine response to fuel-flow disturbance. Altitude, 35,000 feet; Mach number, 0.45.

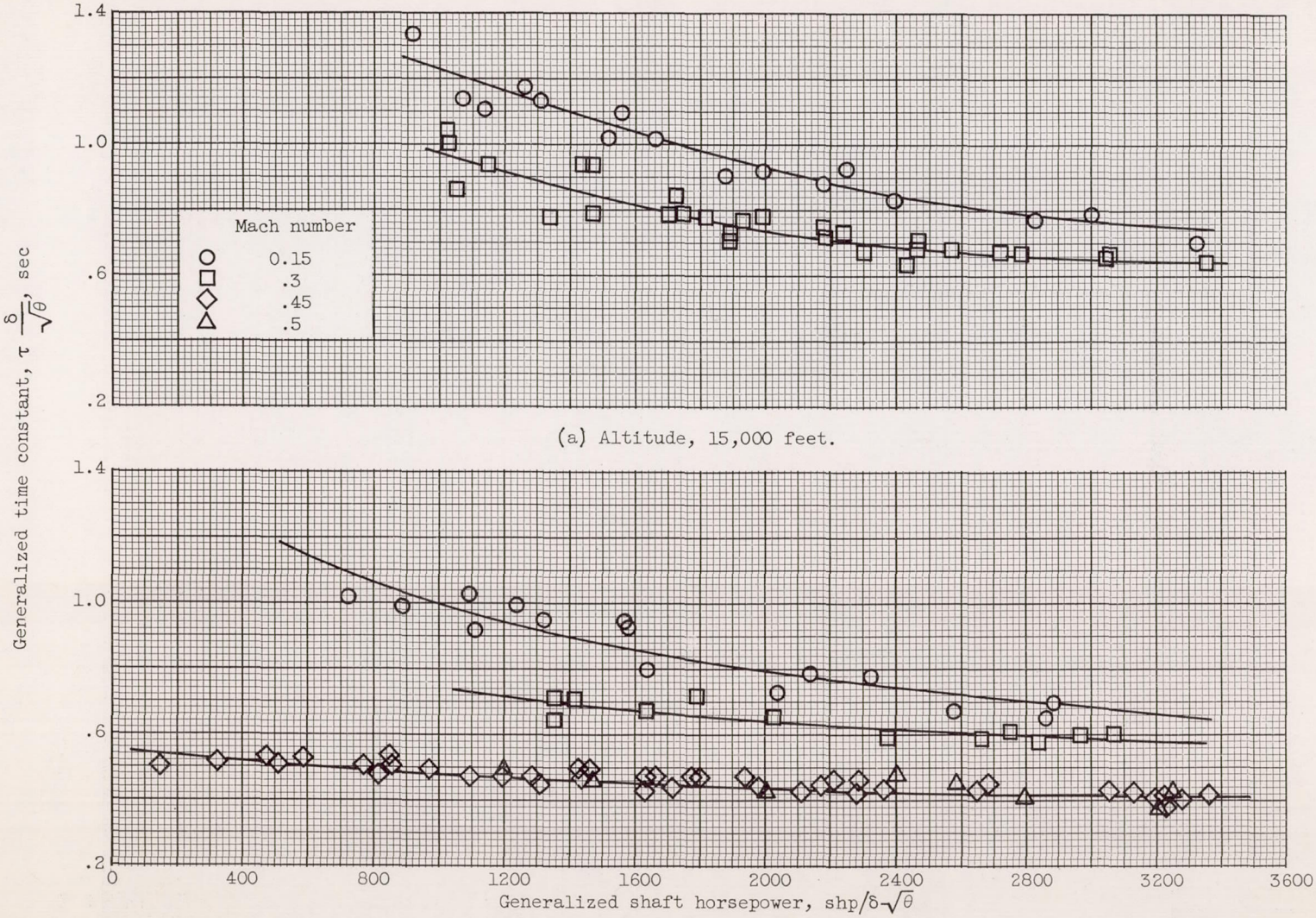

(a) Altitude, 15,000 feet.

(b) Altitude, 35,000 feet.

Figure 6. - Variation of generalized time constant with Mach number and generalized shaft horsepower at two altitudes.

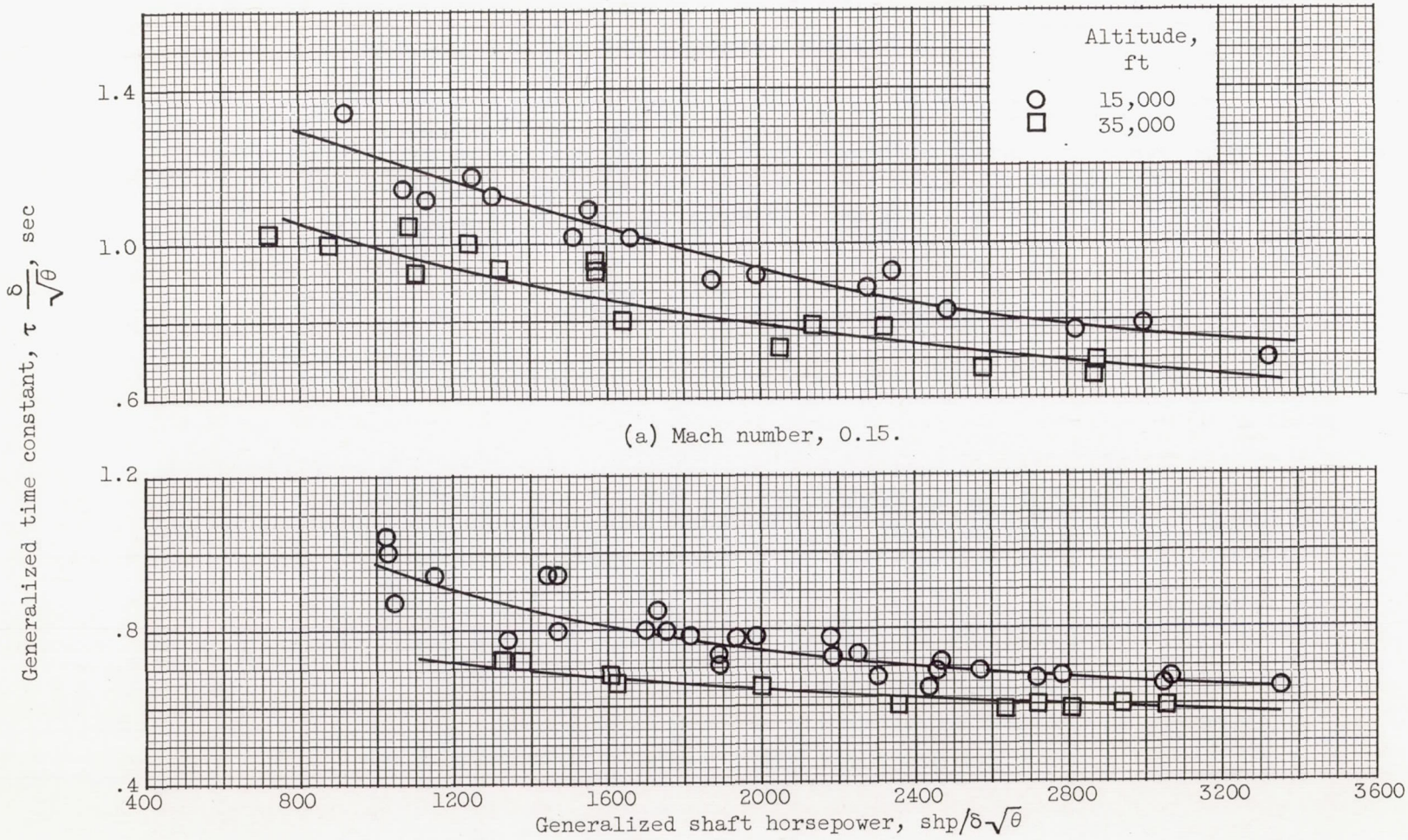

(a) Mach number, 0.15.

(b) Mach number, 0.3.

Figure 7. - Variation of generalized time constant with altitude and generalized shaft horsepower at two Mach numbers.

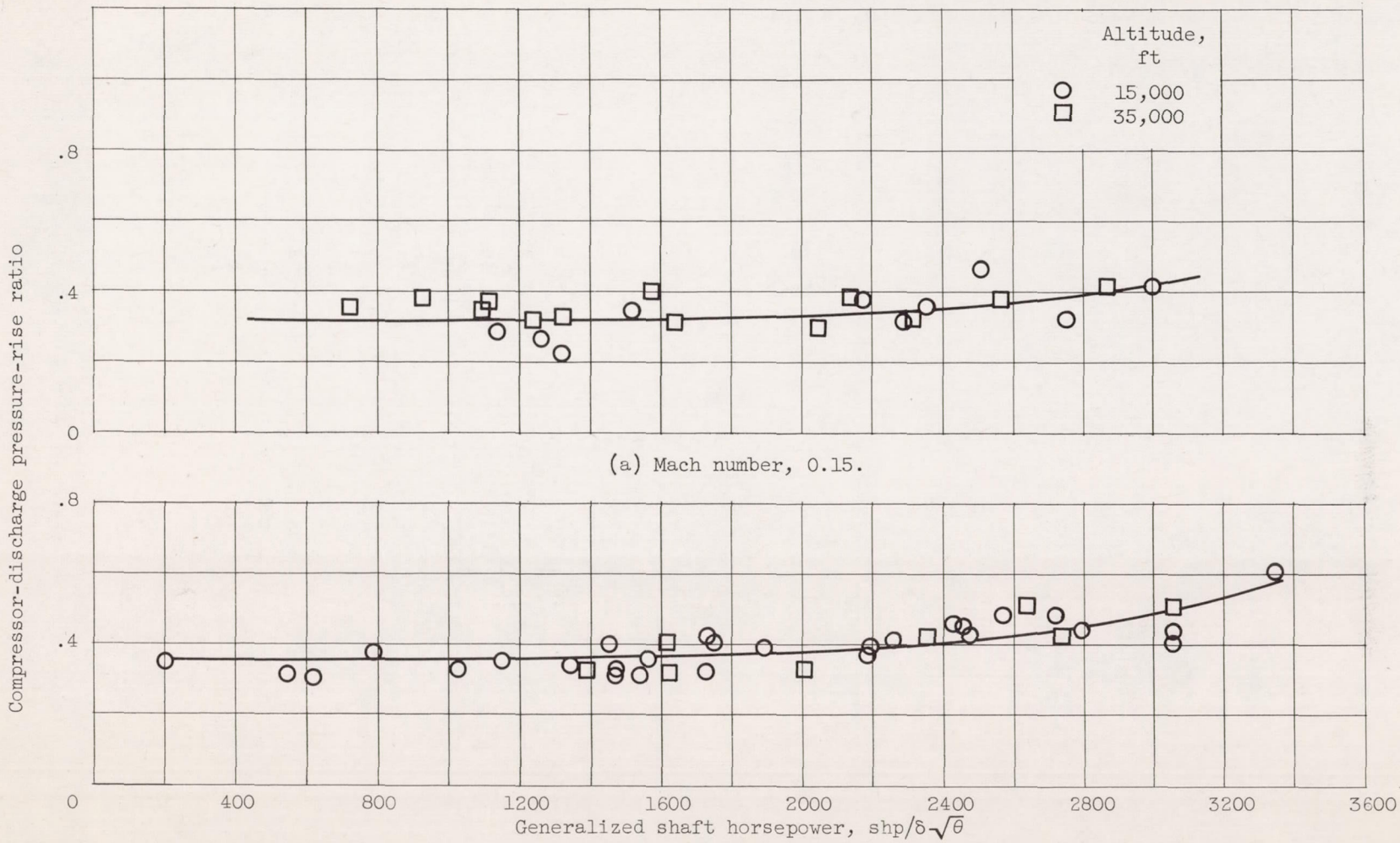

(a) Mach number, 0.15.

(b) Mach number, 0.3.

Figure 8. - Variation of compressor-discharge pressure-rise ratio with altitude and generalized shaft horsepower at two Mach numbers.

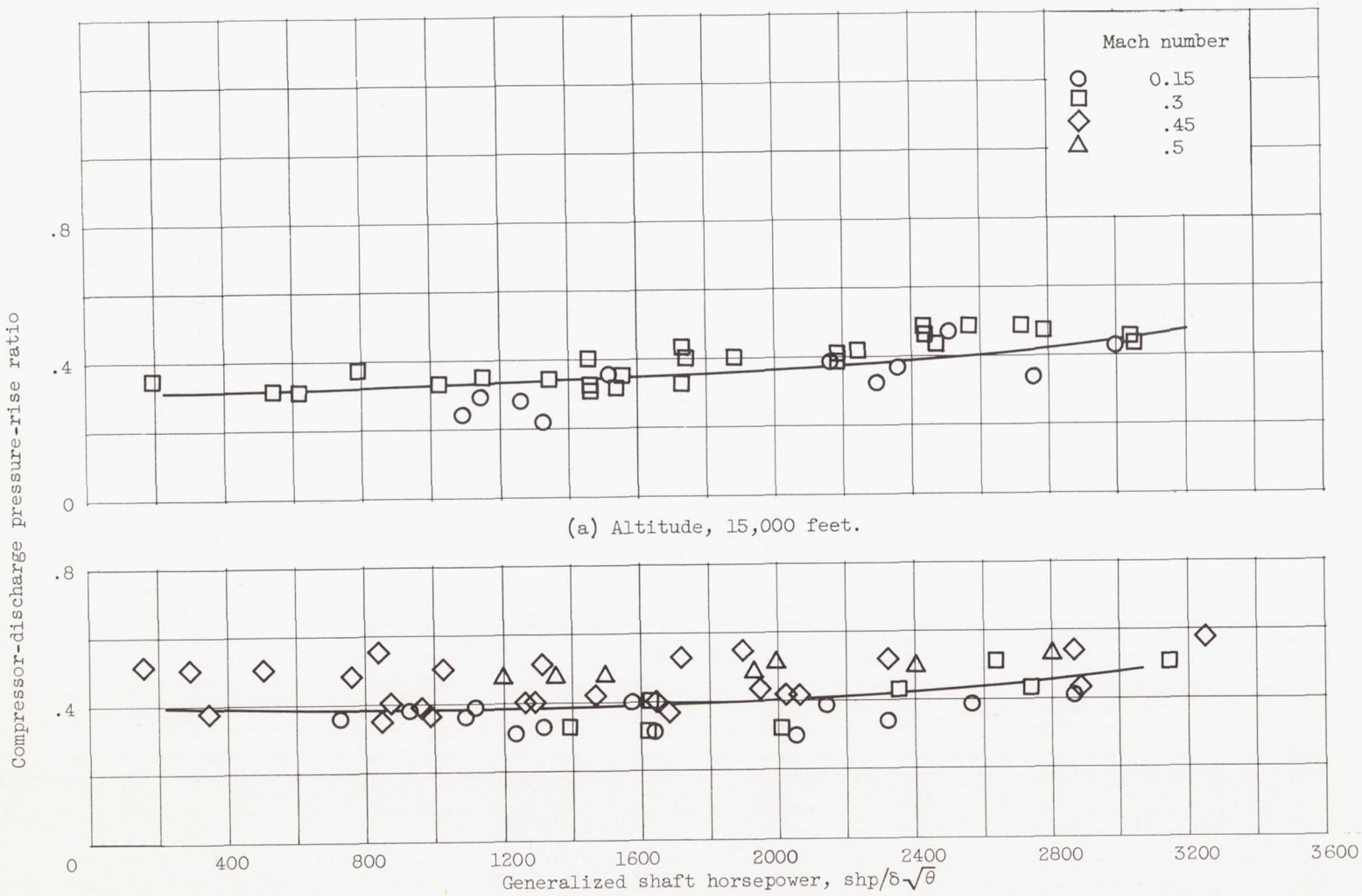

(a) Altitude, 15,000 feet.

(b) Altitude, 35,000 feet.

Figure 9. - Variation of compressor-discharge pressure-rise ratio with Mach number and generalized shaft horsepower at two altitudes.

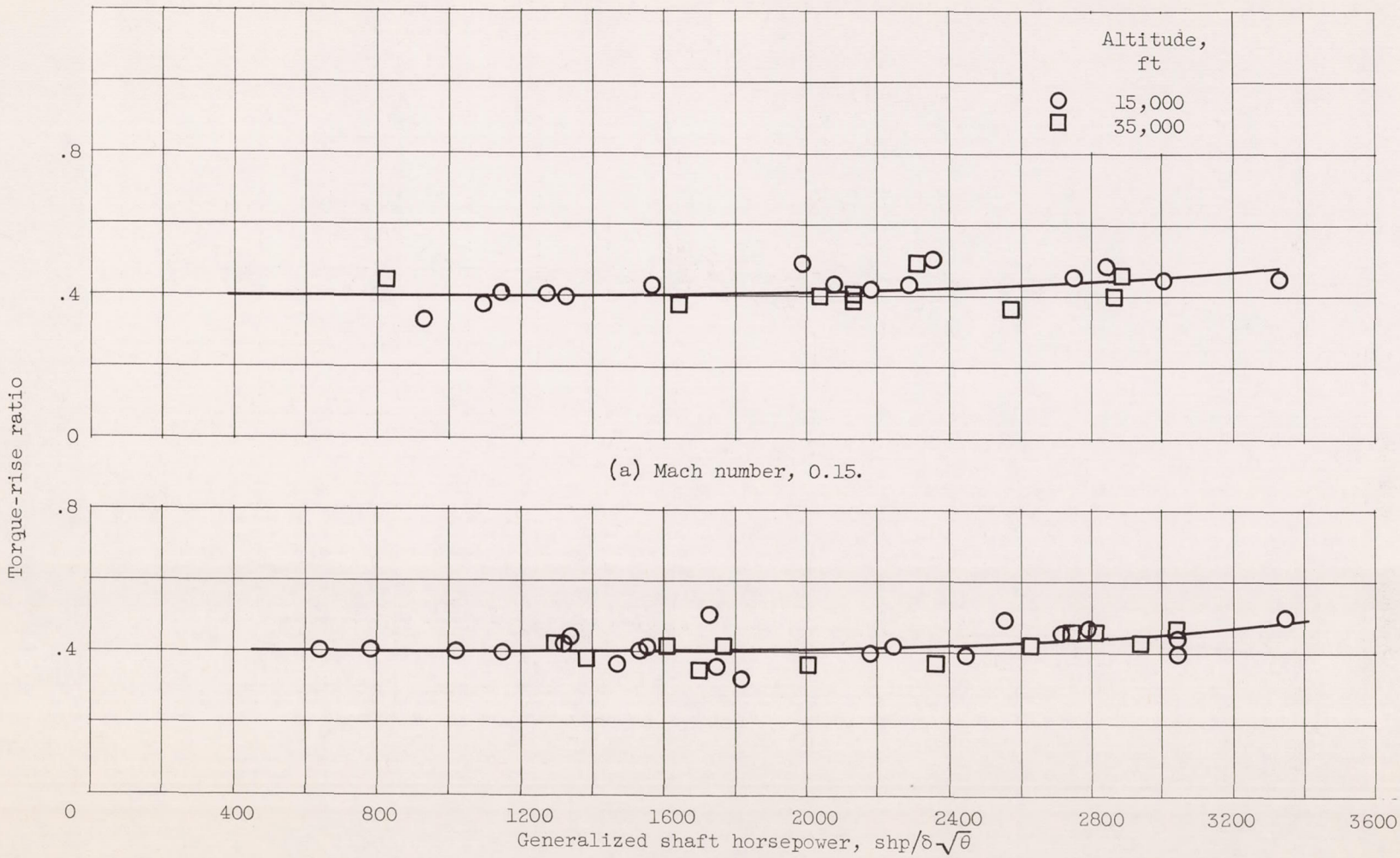

(a) Mach number, 0.15.

(b) Mach number, 0.3.

Figure 10. - Variation of torque-rise ratio with altitude and generalized shaft horsepower at two Mach numbers.

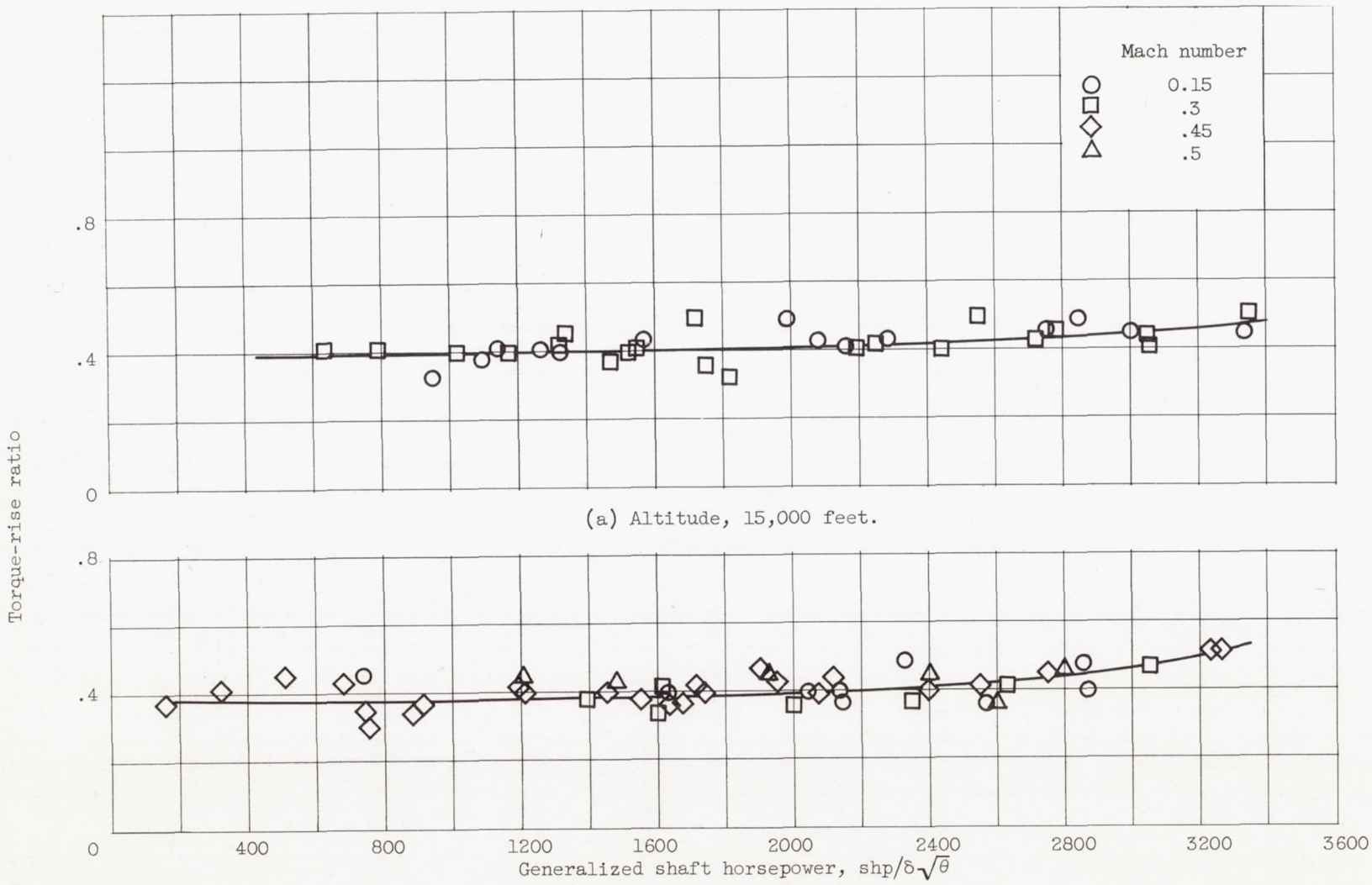

(b) Altitude, 35,000 feet.

Figure 11. - Variation of torque-rise ratio with Mach number and generalized shaft horsepower at two altitudes.

3527

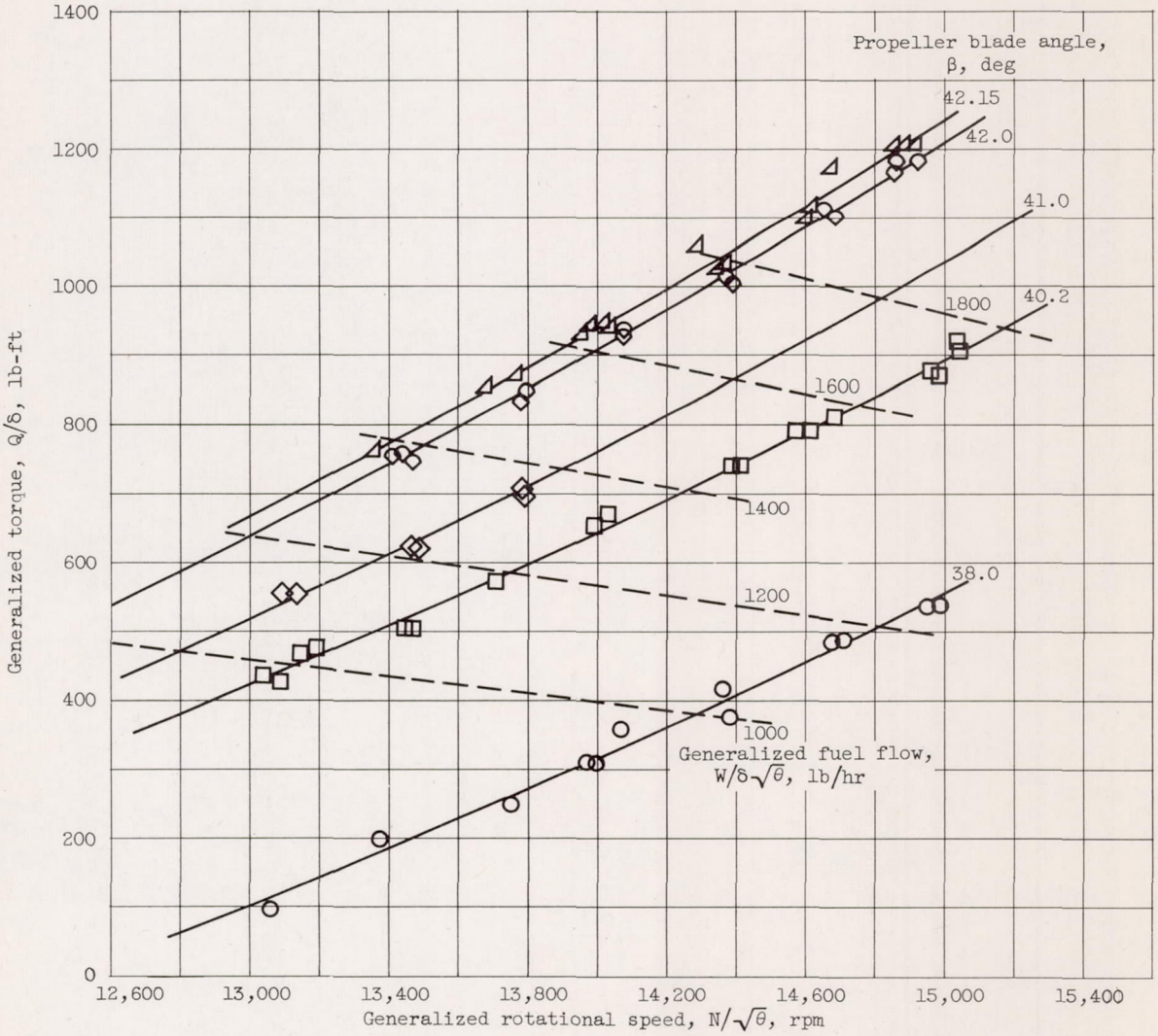

Figure 12. - Variation of generalized torque with generalized engine rotational speed. Altitude, 15,000 feet; Mach number, 0.3.

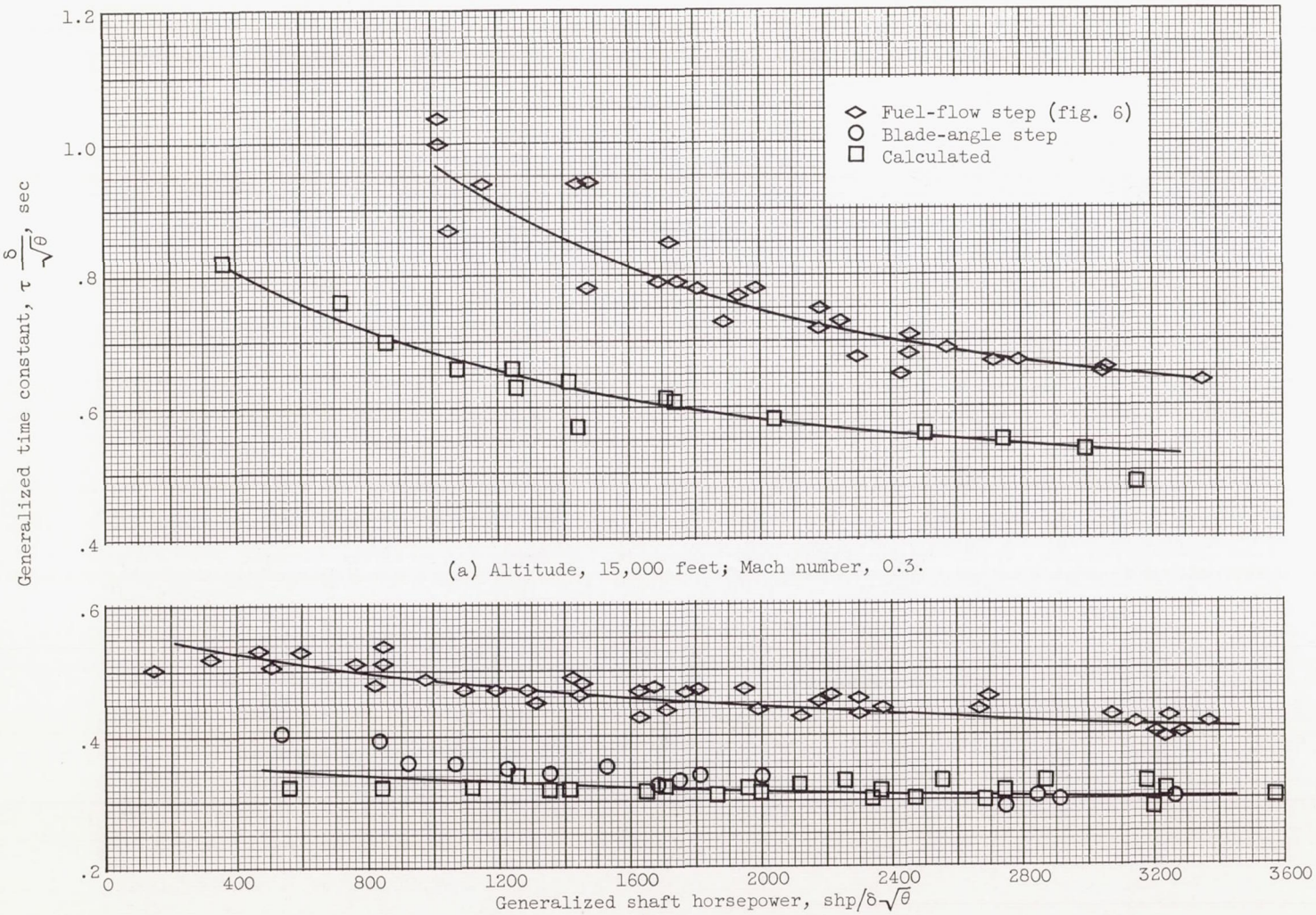

(a) Altitude, 15,000 feet; Mach number, 0.3.

(b) Altitude, 35,000 feet; Mach number, 0.45.

Figure 13. - Comparison of calculated generalized time constant with values obtained from fuel-flow and blade-angle steps.

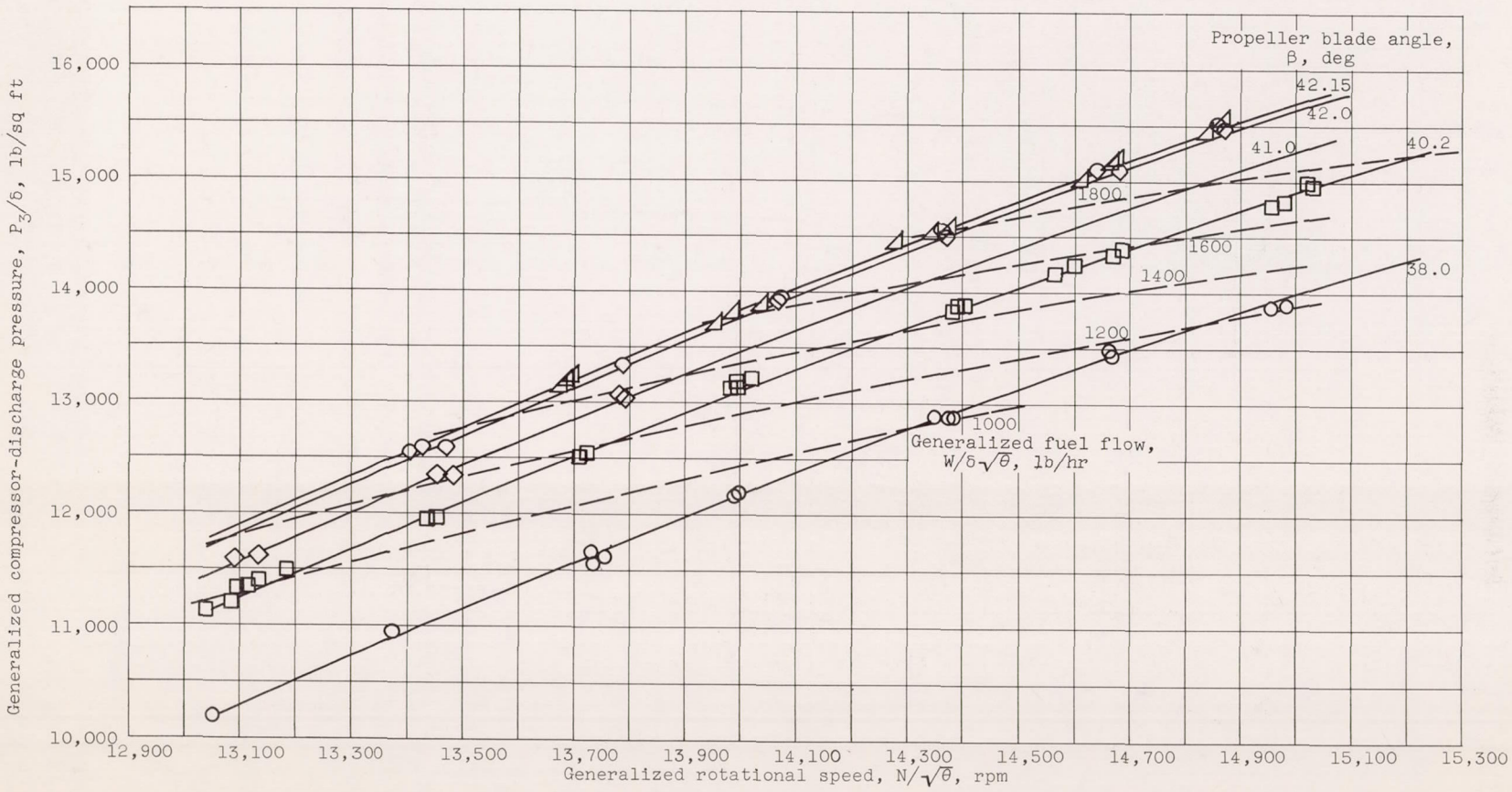

Figure 14. - Variation of generalized compressor-discharge pressure with generalized engine rotational speed. Altitude, 15,000 feet; Mach number, 0.3.

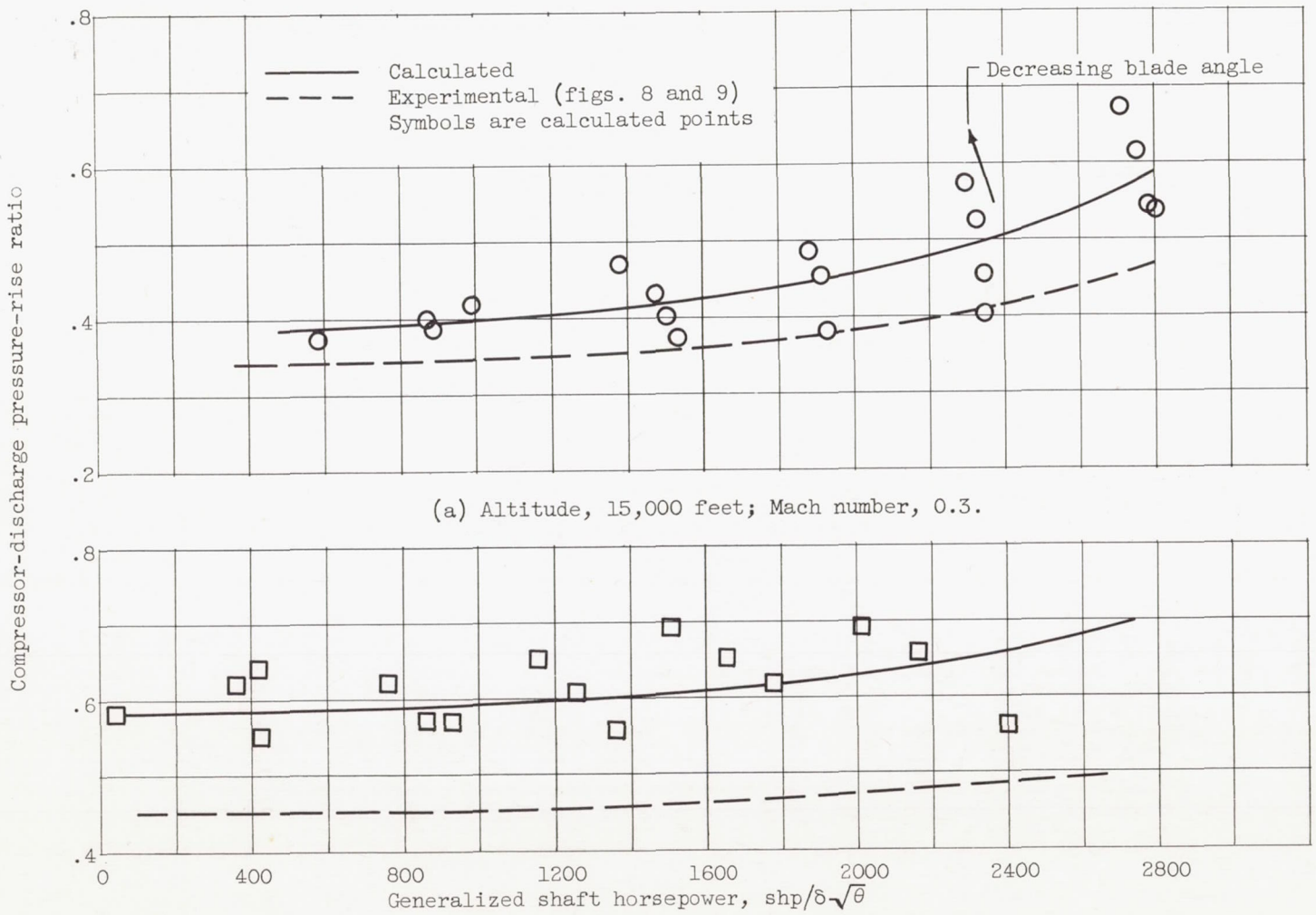

(a) Altitude, 15,000 feet; Mach number, 0.3.

(b) Altitude, 35,000 feet; Mach number, 0.45.

Figure 15. - Comparison of calculated compressor-discharge pressure-rise ratio with values obtained from fuel-flow steps.

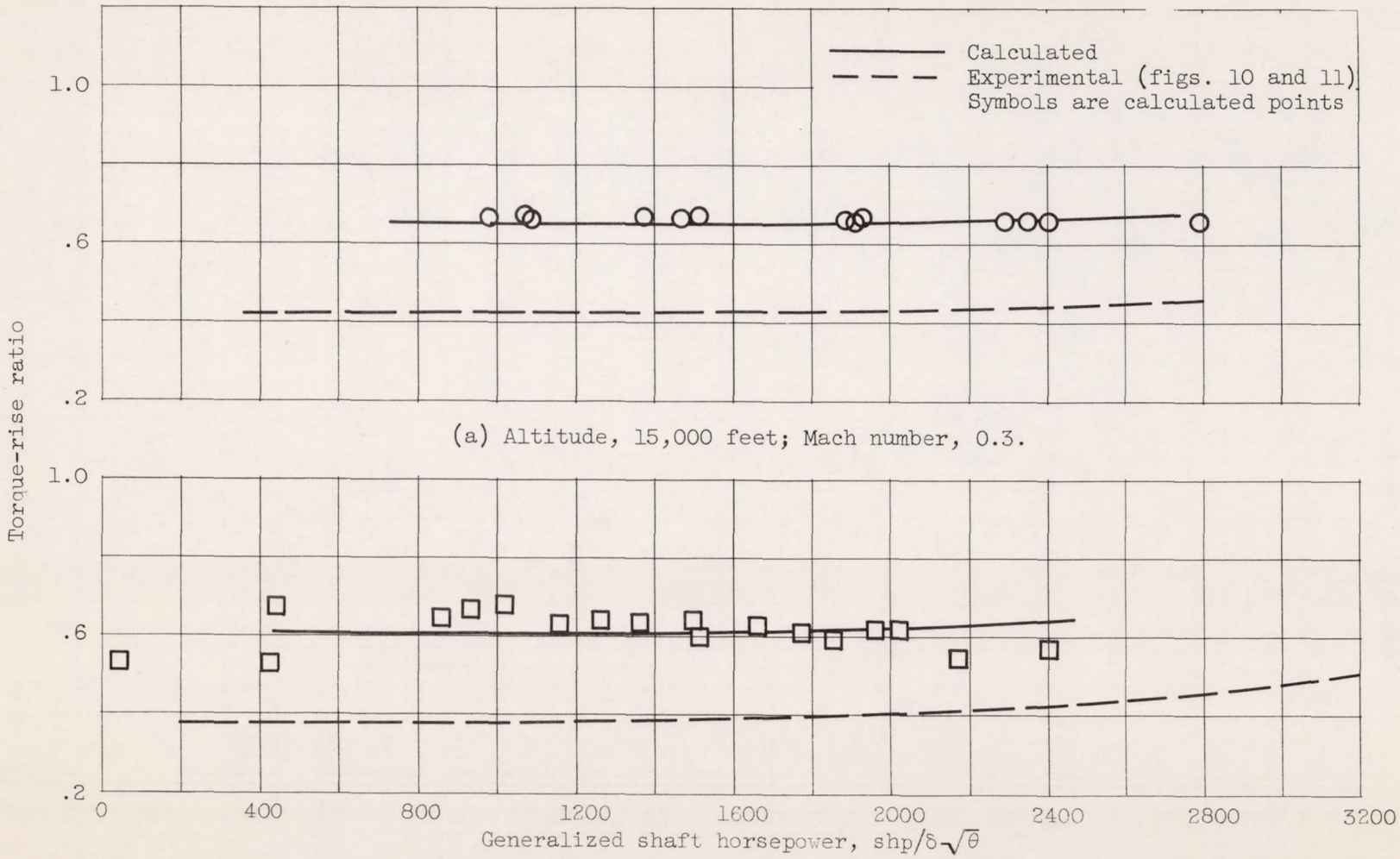

(a) Altitude, 15,000 feet; Mach number, 0.3.

(b) Altitude, 35,000 feet; Mach number, 0.45.

Figure 16. - Comparison of calculated torque-rise ratio with values obtained from fuel-flow steps.

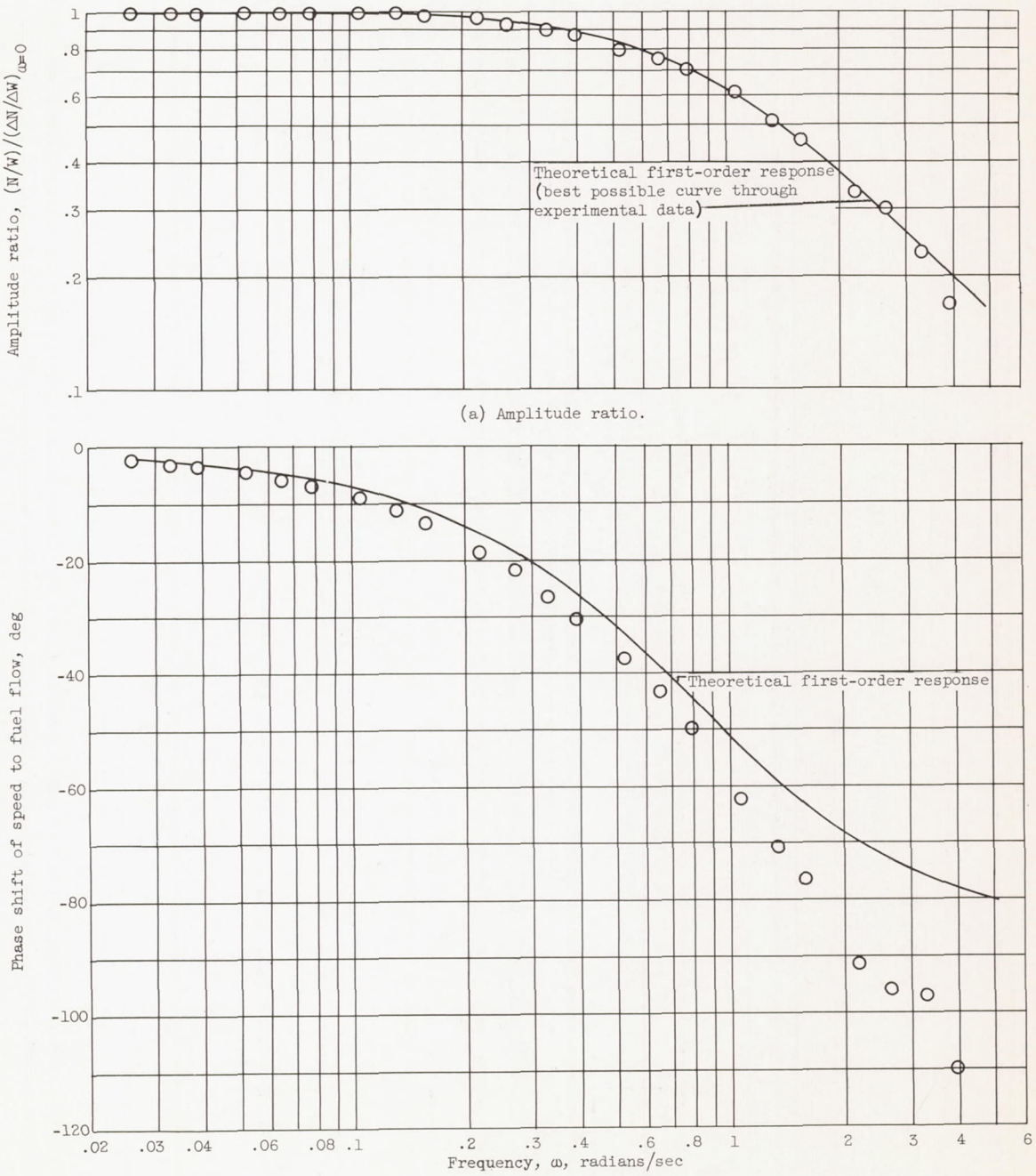

(a) Amplitude ratio.

(b) Phase shift.

Figure 17. - Harmonic analysis of response of engine speed to fuel-flow step. Altitude, 35,000 feet; Mach number, 0.45; change in rotational speed, 6 percent.

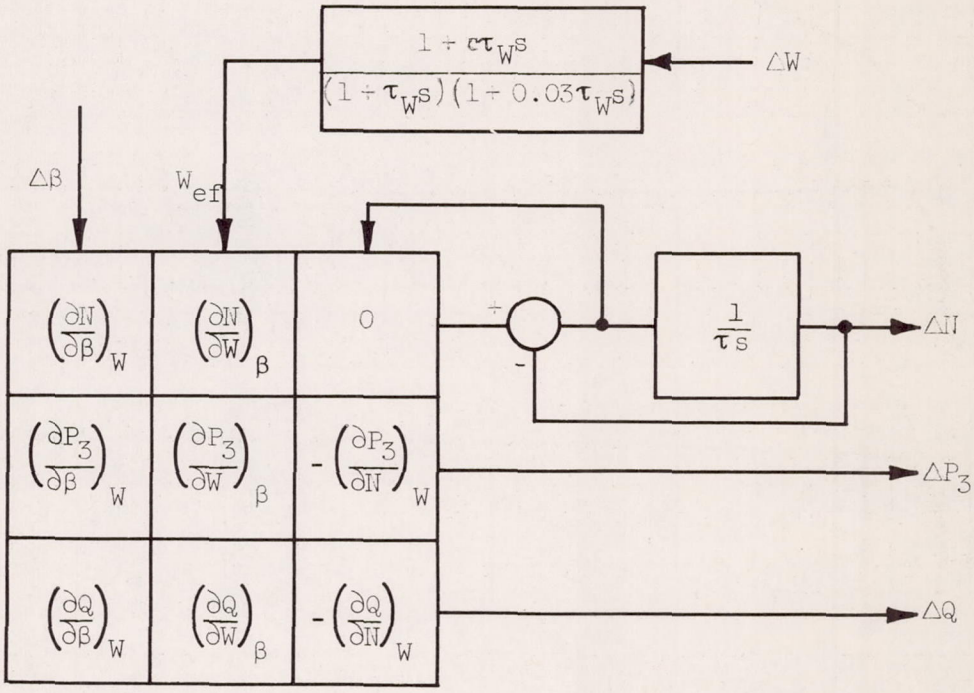

Figure 18. - Matrix form used in description of experimental response of turboprop engine having dynamic relation between fuel input and effective fuel input.

CE-6 back

3527

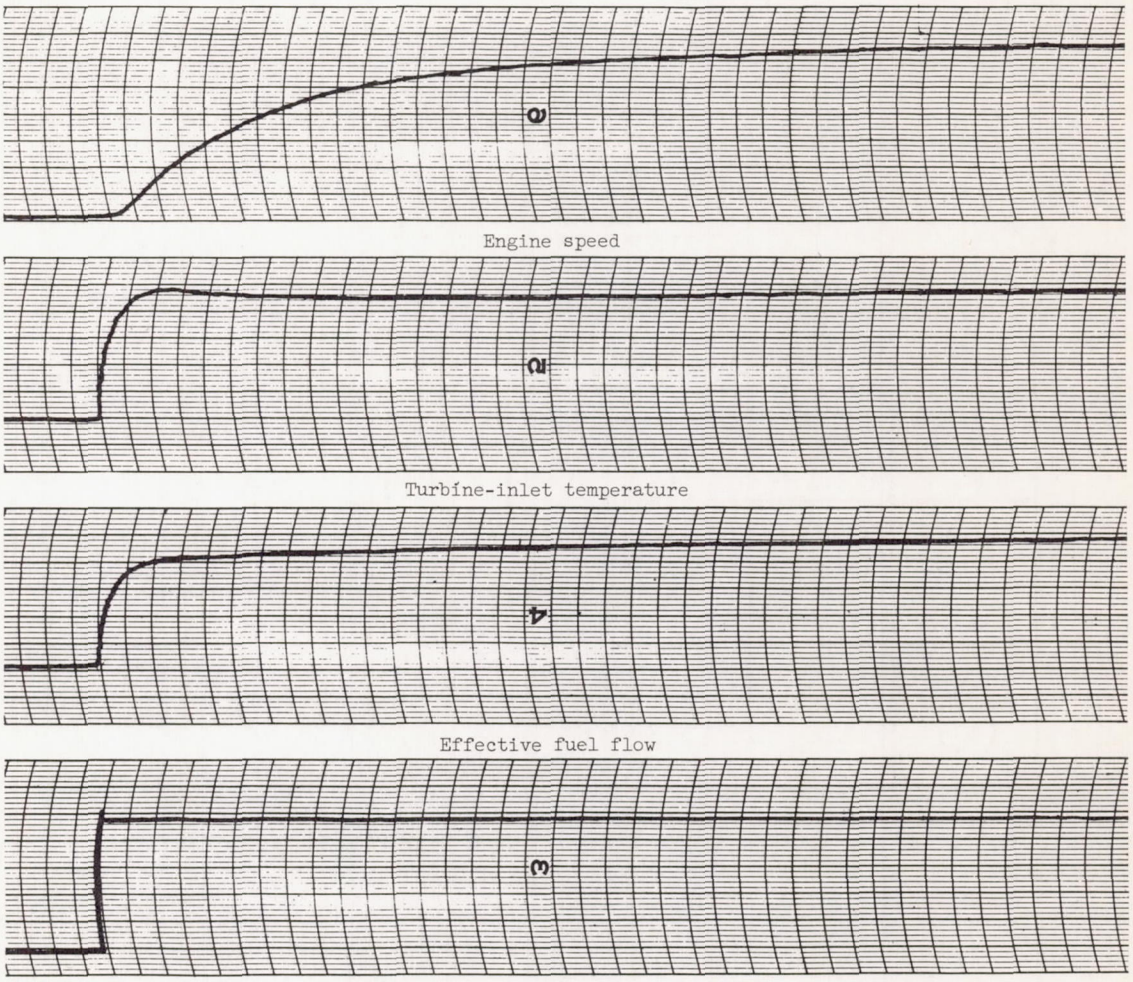

(a) Analog simulation. (Computer set as in fig. 18.)

Figure 19. - Comparison of simulated and experimental engine response to fuel-flow step.

3527

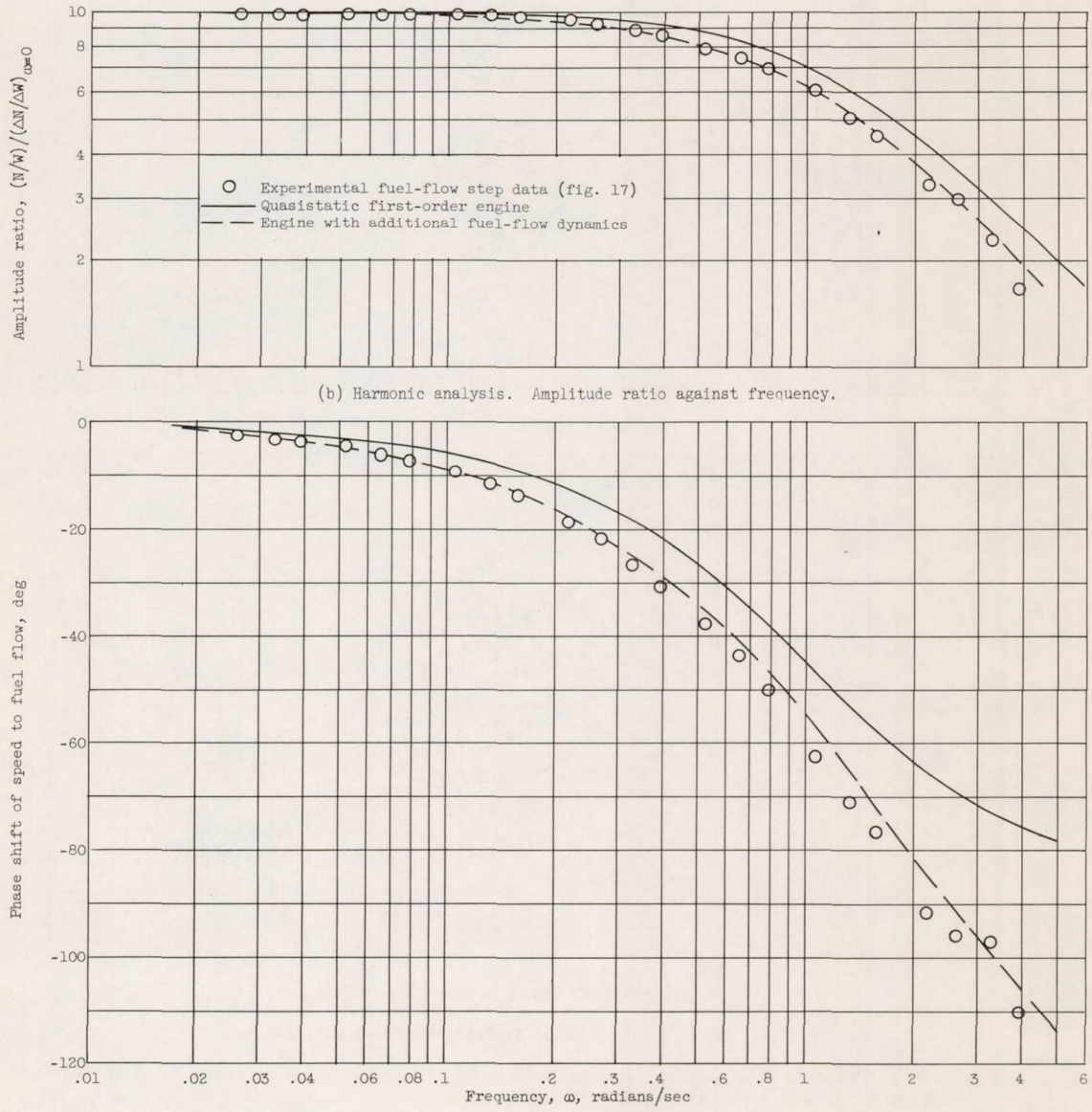

(b) Harmonic analysis. Amplitude ratio against frequency.

(c) Harmonic analysis. Phase shift against frequency.

Figure 19. - Concluded. Comparison of simulated and experimental engine response to fuel-flow step.

3527

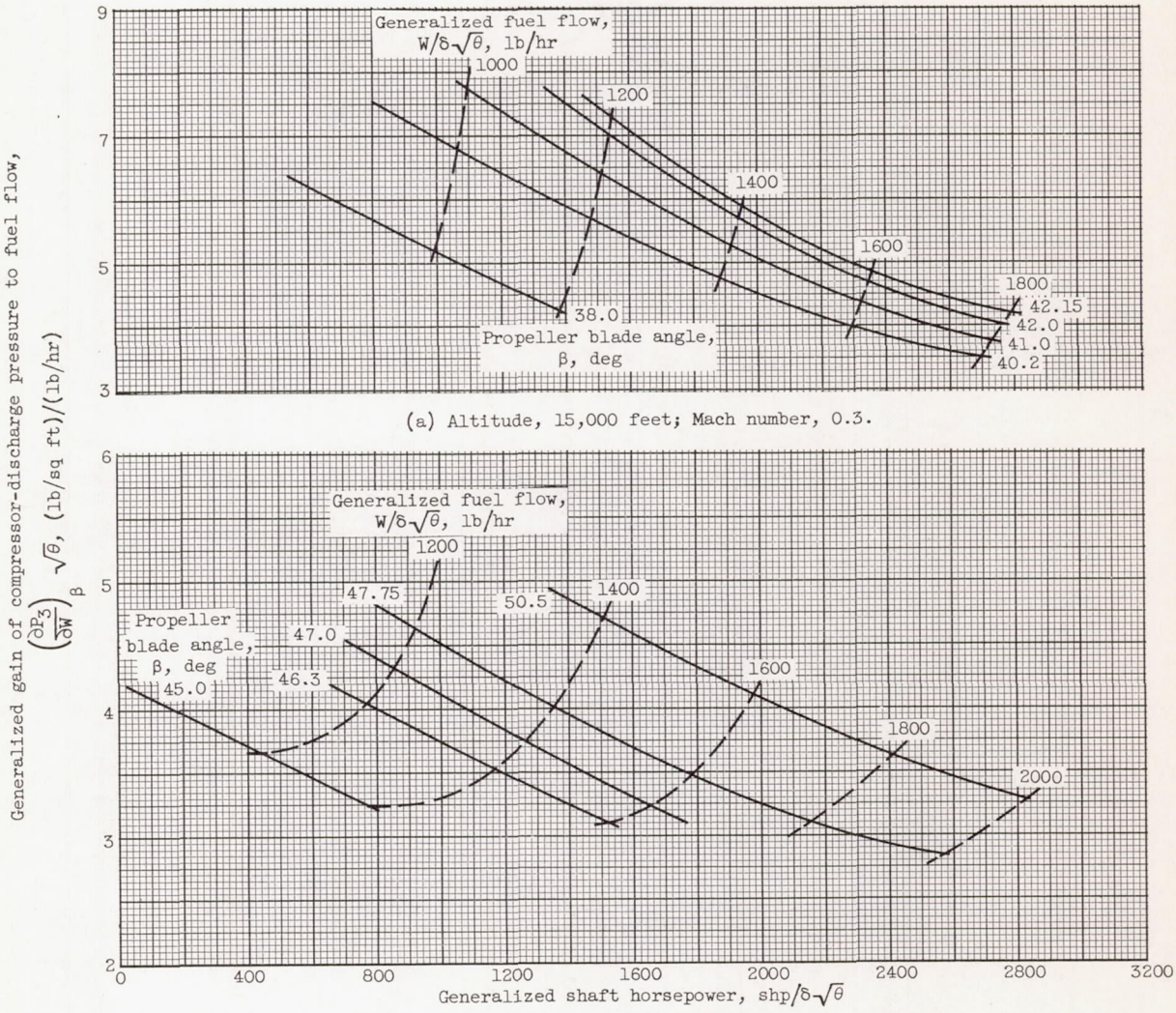

(a) Altitude, 15,000 feet; Mach number, 0.3.

(b) Altitude, 35,000 feet; Mach number, 0.45.

Figure 20. - Comparison of generalized gains of compressor-discharge pressure to fuel flow and propeller blade angle at several flight conditions.

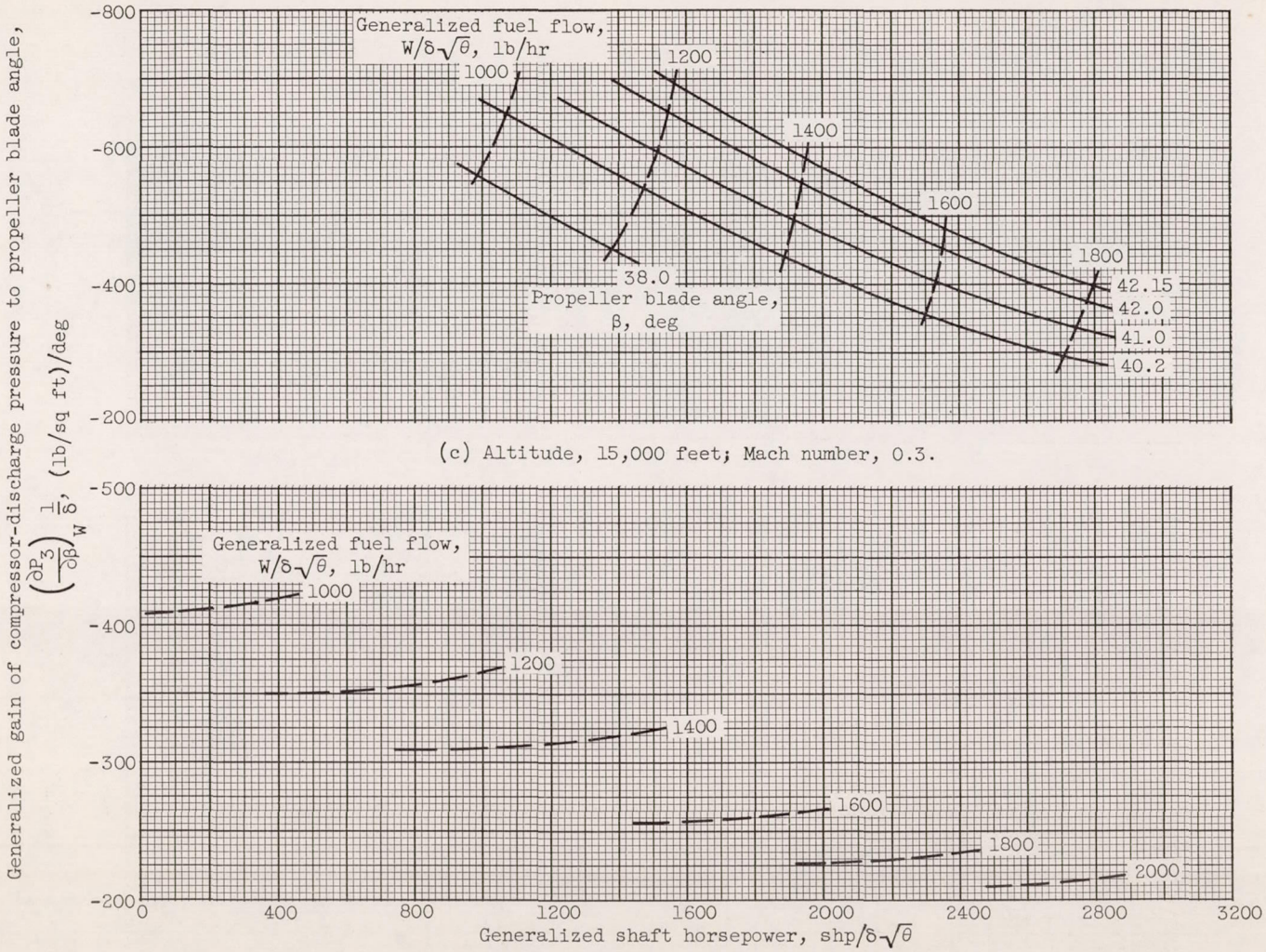

(c) Altitude, 15,000 feet; Mach number, 0.3.

(d) Altitude, 35,000 feet; Mach number, 0.45.

Figure 20. - Concluded. Comparison of generalized gains of compressor-discharge pressure to fuel flow and propeller blade angle at several flight conditions.

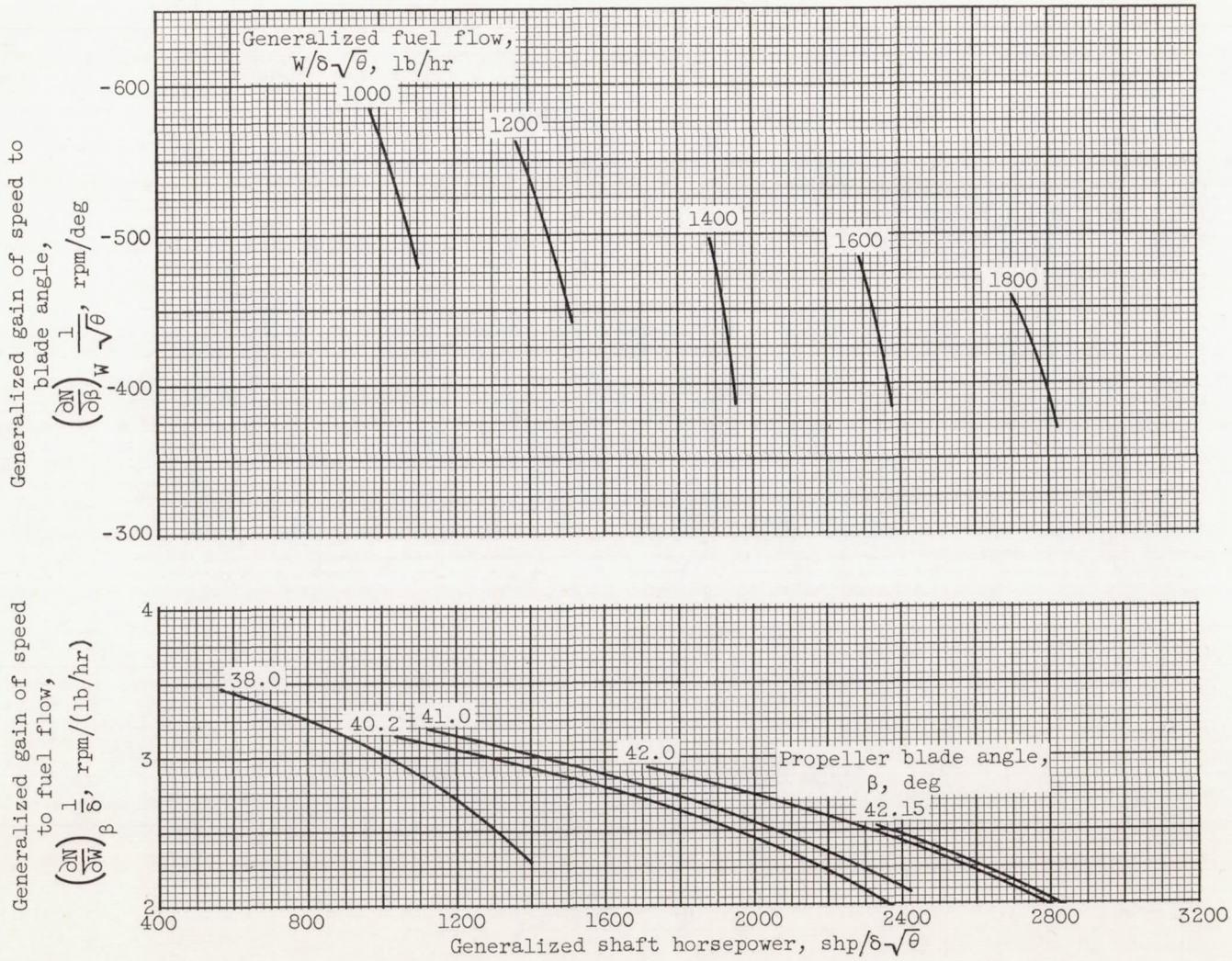

Figure 21. - Variation of generalized gains of speed to propeller blade angle and fuel flow with generalized shaft horsepower. Altitude, 15,000 feet; Mach number, 0.3.

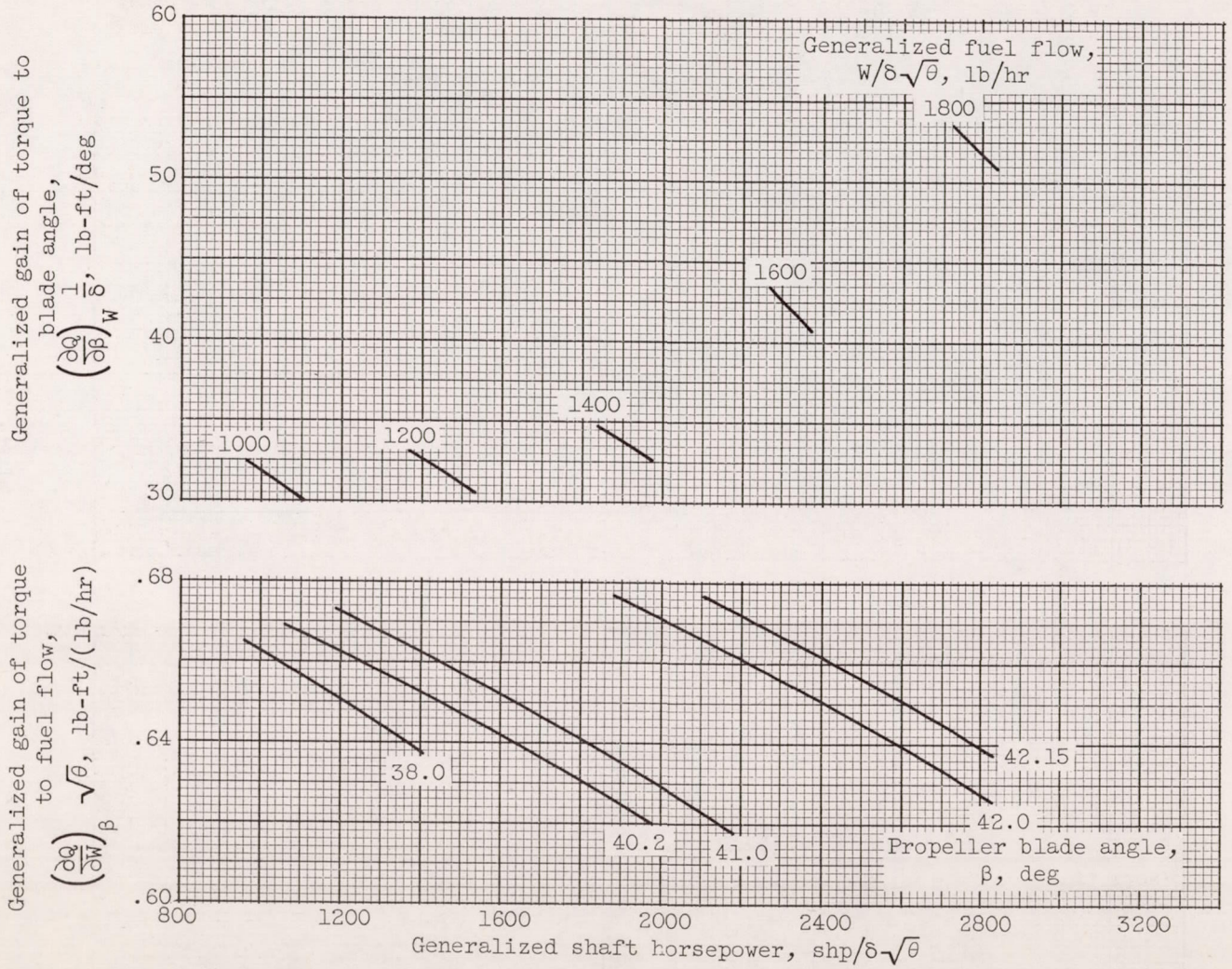

Figure 22. - Variation of generalized gains of torque to propeller blade angle and fuel flow with generalized shaft horsepower. Altitude, 15,000 feet; Mach number, 0.3.

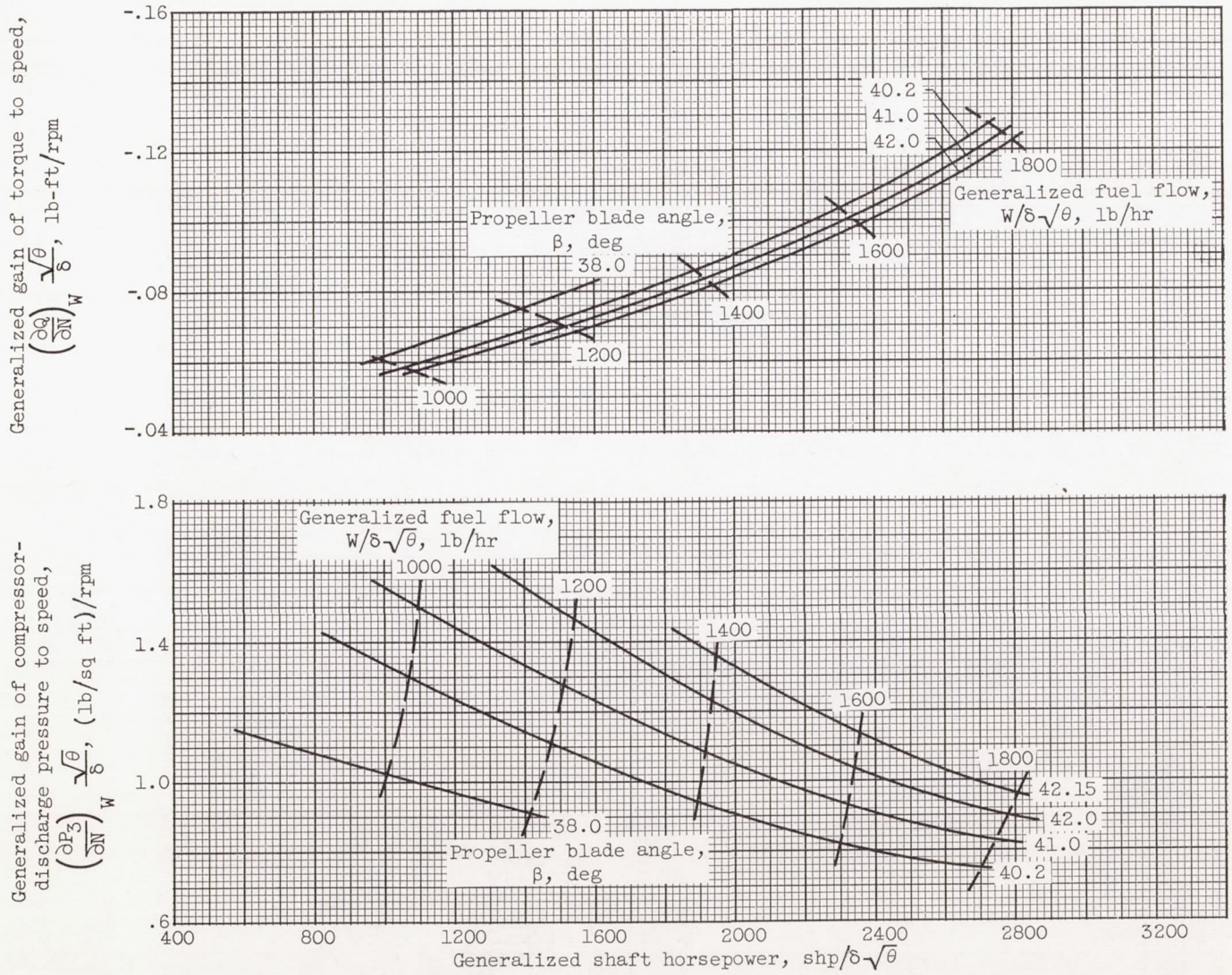

Figure 23. - Variation of generalized gains of torque and compressor-discharge pressure to speed with generalized shaft horsepower. Altitude, 15,000 feet; Mach number, 0.3.